
Reconstruction of a latest Paleocene shallow-marine eutrophic paleoenvironment at Sidi Nasseur (Central Tunisia) based on foraminifera, ostracoda, calcareous nannofossils and stable isotopes ($\delta^{13}\text{C}$, $\delta^{18}\text{O}$)

P. STASSEN^{|1|} C. DUPUIS^{|2|} A.M. MORSI^{|3|} E. STEURBAUT^{|1, 4|} and R.P. SPEIJER^{|1|}

|1| Department of Earth and Environmental Sciences, K.U.Leuven

Celestijnenlaan 200E, B-3001 Leuven, Belgium. Stassen E-mail: peter.stassen@ees.kuleuven.be

Speijer E-mail: robert.speijer@ees.kuleuven.be

|2| Faculté Polytechnique de Mons

9 rue de Houdain, B-7000 Mons, Belgium. E-mail: christian.dupuis@fpms.ac.be

|3| Department of Geology, Faculty of Science

Ain Shams University, 11566 Cairo, Egypt. E-mail: ammorsi@hotmail.com

|4| Department of Paleontology, Royal Belgian Institute of Natural Sciences

Vautierstraat 29, B-1000, Brussels, Belgium. E-mail: etienne.steurbaut@naturalsciences.be

ABSTRACT

In order to unravel faunal and paleoenvironmental parameters in shallow marine settings prior to the Paleocene-Eocene thermal maximum, we investigated the Sidi Nasseur section (NAS) in Central Tunisia. This section exposes Paleocene to lower Eocene shales and marls of the El Haria Formation. The uppermost Paleocene part of the Sidi Nasseur section is marked by poor to moderately rich, but fairly diversified nannofossil associations, containing the typical latest Paleocene taxa of the top of NP9a. The ostracode record displays an almost continuous record in the uppermost Paleocene part of the section. Representatives of *Aegyptiana*, *Paracosta*, *Reticulina* and *Reymenticosta* make up the major part of the ostracode fauna. The benthic foraminiferal assemblage consists of numerous small calcareous benthic foraminifera, like *Anomalinoidea midwayensis* and *Lenticulina* spp. and many large *Fronicularia phosphatica*, *Pyramidulina* spp. These, together with the non-calcareous agglutinated foraminifera and the rare planktic foraminifera, indicate an inner neritic to coastal environment with eutrophic conditions, regularly interrupted by oxygen deficiency. The dominance of non-calcareous benthic foraminifera between intervals with abundant calcareous benthic foraminifera suggests post-mortem dissolution. The foraminiferal $\delta^{13}\text{C}$ record (based upon *Pyramidulina latejugata*) of the latest Paleocene in the Sidi Nasseur area is very similar to these from coeval sediments at Gebel Duwi and Gebel Aweina in Egypt. Oxygen isotopic ratios indicate a marine setting with a water composition affected by evaporation. During the latest Paleocene, the highly productive shallow water environment evolved to shallower water depths with higher salinity and increasing dominance of *A. midwayensis*.

KEYWORDS | Stratigraphy. Benthic foraminifera. Ostracoda. Calcareous nannofossils. Inner neritic. Coastal. Stable isotopes.

INTRODUCTION

The Paleogene has become appreciated as a climatically highly dynamic period with the transition from a near ice-free world to the glacially dominant world of the Neogene (Zachos et al., 2001). Imbedded within long-term Paleogene climate changes are certain key intervals recognized as times of rapid climate change, such as the Paleocene-Eocene thermal maximum (PETM). High-resolution isotopic records of deep-sea sequences are revealing details of these Paleogene climate transitions. In addition, detailed records of biotic responses in continental margins can provide further insights in Paleogene paleoceanographic changes and climate dynamics. In Tunisia are thick and widespread deposits of early Paleogene age, rich in microfossils, exposed and these reveal details of Paleogene stratigraphy and paleoenvironments (e.g., Aubert and Berggren, 1976; Kouwenhoven et al., 1997; Guasti et al., 2006). These sediments were deposited in the southern part of the Tethys Ocean, what was once an extensive east-west tropical seaway connecting the Atlantic and Pacific Oceans during the Mesozoic and early Cenozoic. Much attention has been paid to faunal assemblages and paleoecological aspects of the El Haria Formation (Fm) because it offers a nearly continuous stratigraphic record of the Paleocene. Outcrops of the El Haria Fm near El Kef are well known and distribution patterns of ostracodes (Peypouquet et al., 1986); benthic foraminifera (Kouwenhoven et al., 1997) and dinoflagellates (Guasti et al., 2005) have been intensively studied. These studies indicate an evolution from an initially oligotrophic open and deep marine setting towards a more eutrophic inner neritic setting during the late Paleocene with periods of decreased oxygenation and they suggest that coastal upwelling could have influenced the eutrophication in the El Kef area.

In order to unravel the nature and spatial distribution of eutrophic conditions in the southern Tethys, we focus on paleoenvironmental characteristics of the Sidi Nasseur (NAS) section, a Paleocene shallow marine sequence, 50 km to the southwest of El Kef. We discuss the uppermost Paleocene part of this section in detail, since this allows us to build a baseline of faunal distribution patterns and paleoenvironmental settings in the southern Tethys prior to the PETM. We particularly focus on the benthic foraminiferal record, which provides insight into parameters such as water depth, trophic conditions and oxygenation. Additional information is provided by the quantitative distribution of calcareous nannofossils, stable isotopic (C, O) data and a qualitative assessment of the ostracode assemblages. The faunal sequence into the overlying PETM beds is part of an ongoing research on a new high-resolution sample set collected in 2006.

GEOLOGICAL SETTING

In northwest Tunisia, the easily eroded clays and marls of the El Haria Fm form wide valleys and plains, creating excellent opportunities for studies on early Paleogene events. The Maastrichtian to lower Ypresian El Haria Fm overlies Campanian-Maastrichtian limestones of the Abiod Formation and is overlain by Ypresian phosphatic limestones of the Metlaoui Formation (Fig. 2). The El Haria Fm consists mainly of dark grey fissile shales and marls with thin intercalations of limestones particularly in the Danian part. The occurrence of gypsum veins is common in the Paleocene part, while phosphatic levels are mostly restricted to the top of the formation (Aubert and Berggren, 1976). The lower and middle Paleocene part of the El Haria Fm is transgressive (zones P2 and P3), extending over a large part of Tunisia and, in the Tunisian Trough, is followed by a general shallowing trend during the late Paleocene (zones P4 and P5) (Aubert and Berggren, 1976; Kouwenhoven et al., 1997; Guasti et al., 2005). Foraminifera, ostracoda and dinoflagellate studies indicate that the environment at El Kef evolved from an open marine outer neritic-upper bathyal setting towards an inner neritic setting during the late Paleocene (Donze et al., 1982; Peypouquet et al., 1986; Kouwenhoven et al., 1997; Guasti et al., 2005).

Lateral facies and thickness variations in the El Haria Fm are thought to be structurally controlled along basement lineaments resulting in a number of small tectonically controlled basins (Zaïer et al., 1998). The large

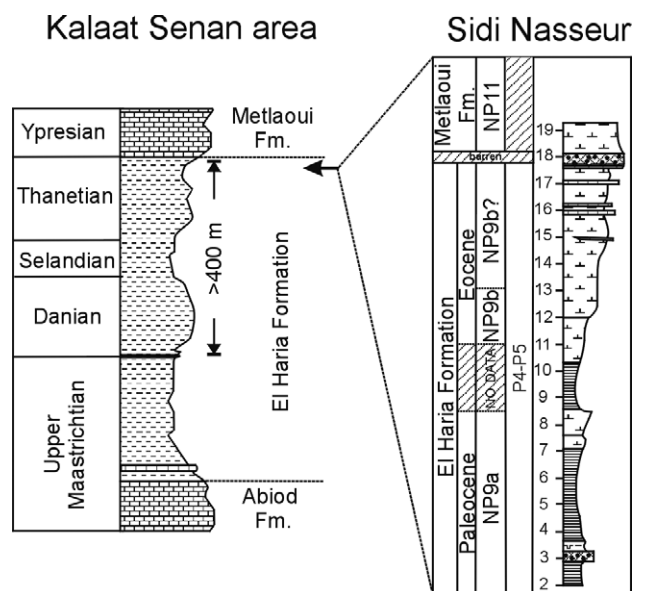


FIGURE 2 | Lithology and stratigraphy of El Haria Formation at Kalaat Senan area and Sidi Nasseur section. Planktic foraminifera biostratigraphy is based on Berggren and Pearson (2005) using the distribution of *M. velascoensis*; calcareous nannofossil biostratigraphy on Martini (1971) and Aubry (1999).

emerged zone of the Kasserine Island (Central Tunisia) separated the northern and southern basins (Zaïer et al., 1998). The result (Fig. 1) is a latest Cretaceous-Paleocene paleogeography characterized by subsiding troughs in the north and northeast (NW Tunisian Trough and NE Tunisian Basin) and the Gafsa Gulf in the southwest (Aubert and Berggren, 1976; Zaïer et al., 1998; Bensalem, 2002). During the Paleocene, the Kalaat Senan region was situated in the southern proximal part of the subsiding Tunisian Trough and in the vicinity of the emerged Kasserine Island. Prolonged marine sedimentation took place in a neritic setting with high subsidence rate and high sediment input, and with reduced sediment thickness towards the Kasserine Island (Bensalem, 2002).

MATERIAL AND METHODS

This study is based on a multidisciplinary approach, including micropaleontology, sedimentology and geochemistry. The Sidi Nasseur (NAS) section is located close to Kalaat Senan, 50 km to the southwest of El Kef. The studied section forms the top part of an expanded and well-exposed Maastrichtian-Ypresian sequence of the El Haria Fm (Dupuis, pers. comm.). This area has been the subject of various research activities on the Cretaceous/Paleogene and Danian/Selandian boundaries (Steurbaut et al., 2000; Dupuis et al., 2001; Guasti et al., 2006; Van Itterbeeck et al., 2007). Study of the uppermost Paleocene and lower Eocene part of the El Haria

Fm in the Kalaat Senan area is generally more complicated than the lower boundaries because of the lower degree of exposure and the presence of faults. The Sidi Nasseur section, east of the Sidi Nasseur hilltop, is a rare exception to this general rule, presenting a non-faulted expanded Paleocene/Eocene boundary sequence. The base of the analyzed section is taken just beneath a distinct phosphatic layer. Such phosphatic intervals are useful marker beds as they can be traced to nearby outcrops. The section terminates where the dip of the slope decreases and the surface is covered by debris. In this report, we discuss the uppermost Paleocene part of the well-exposed section.

Calcareous nannofossils provide the main biostratigraphic framework for the studied section. Planktic foraminifera are too rare to provide any additional detail. Washed residues were obtained following conventional procedures. About 80 grams of sediment were dried at 50–60°C for 24 hours or longer and afterwards soaked in a Na₂CO₃ solution for a day. After disintegration, the samples were washed over a 63 µm sieve and dried at 50–60°C; this treatment was repeated twice whenever the washed residues remained somewhat aggregated. After complete disaggregation, the dried residues were sieved into three fractions (63–125 µm, 125–630 µm, >630 µm). A representative split for quantitative analysis (approximately >300 benthic specimens) was obtained from the 125–630 µm fraction using a microsplitter. From these splits, all benthic specimens were picked, identified, counted and permanently stored on micropaleontological

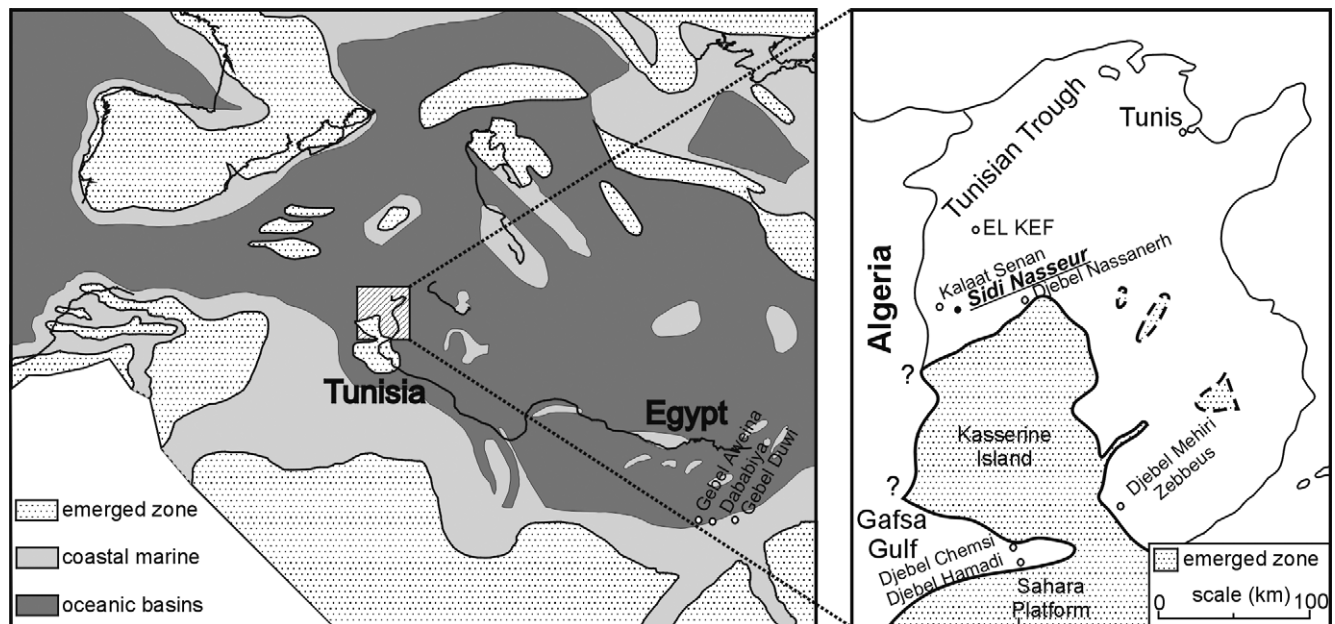


FIGURE 1 | Paleogeographical reconstruction of Tunisia during the deposition of the El Haria Formation (upper Maastrichtian to lower Eocene) and location of the investigated Sidi Nasseur section (modified from Dercourt et al., 2000 and Saint-Marc and Berggren, 1988 after Burollet, 1967).

slides. Benthic foraminiferal numbers (numbers/gram sediment) were calculated for the 125–630 μm fraction. Paleoproductivity levels and dissolution horizons are reflected by changes in numbers foraminifera per gram sediment and can be quantified as foraminiferal accumulation rates (numbers per cm^2 per ka). Because of the lack of accurate time control in the section, foraminiferal numbers are used instead. Relative abundances are expressed as the proportion (percentage) of a species in the entire assemblage and foraminiferal numbers are expressed as the numbers of individuals per gram of sediment. Additional material from the $>250 \mu\text{m}$ fraction was scanned quantitatively for less frequent large species (e.g., *Pyramidulina* spp. and *Frondicularia phosphatica*). Larger specimens of *Pyramidulina* spp. (*Nodosaria* spp., according to older literature) were often broken but easily recognizable. All specimens with two or more connected chambers were counted.

Carbonate contents of the bulk sediment were measured in the Laboratoire de Géologie fondamentale et appliquée de la Faculté Polytechnique de Mons. The pulverized bulk material (0.5 to 2 gram) was dissolved in a 10% hydrochloric acid. The obtained volumes CO_2 gas could be calibrated with the same reaction of 0.5 gram pure CaCO_3 . Foraminiferal $\delta^{13}\text{C}$ and $\delta^{18}\text{O}$ records are based upon single specimens of thick-shelled *Pyramidulina latejugata* and a few *Frondicularia phosphatica* specimens. We analyzed these large nodosariids instead of the more commonly used *Cibicides* or *Cibicidoides*, because it was not possible to separate the diagenetic infillings from the shells of the latter taxa. Clean well-preserved nodosariids were selected and, where present, their diagenetic infillings were separated from the tests by crushing and hand-picking (cf. Schmitz et al., 1996; Charisi and Schmitz, 1998). Carbon and oxygen isotope analyses were performed with a Kiel III carbonate preparation line connected online to a ThermoFinnigan 252 mass spectrometer at the University of Erlangen. $\delta^{13}\text{C}$ and $\delta^{18}\text{O}$ are given in permil relative to V-PDB. Analytical reproducibility for carbon and oxygen isotope analyses was better than $\pm 0.06\text{‰}$ (1 std. dev.).

STRATIGRAPHY

The NAS section represents an expanded upper Paleocene/lower Eocene boundary sequence. Microfossil associations (calcareous nannofossils and benthic foraminifera) allow a subdivision of the Sidi Nasseur section into an uppermost Paleocene sequence and a lowermost Eocene sequence. The lower part (from 2.75 m to 10.0 m) consists of typical upper Paleocene benthic foraminiferal and nannofossil assemblages.

Lithology

The Paleocene sequence (from base to 10.0 m, Fig. 2) consists of dark grey to brownish shales with occasional more calcareous intervals. A 50 cm thick brownish layer of a more indurated calcareous phosphatic bed with numerous coprolites is intercalated at the base. Several levels contain shark and fish teeth and coprolites, but macro-invertebrate remains have not been observed. Calcareous clay grading into marl with thin limestone intercalations, conformably overlies the Paleocene sequence.

Biostratigraphy

Calcareous nannofossil Biostratigraphy

Calcareous nannofossil assemblages (up to 8.50 m) are marked by a high diversity in Discoasteraceae (*Discoaster multiradiatus*, *D. falcatus*, *D. nobilis* and *D. salisburgensis*), Fasciculithaceae (*Fasciculithus alanii*, *F. involutus*, *F. schaubii* and *F. sidereus*) and *Toweius* (*T. eminens*, *T. pertusus* and *T. serotinus*). The co-occurrence of these taxa in association with the presence of *Pontosphaera* and absence of the genus *Tribrachiatus* refers to the top of nannofossil zone NP9a (sensu Aubry, 1999; also in Dupuis et al., 2003). The interval contains fairly rich associations both in terms of number of specimens (mean value 50 nannoliths per 10 mm^2 , Fig. 3) as well as species diversity (~ 20 taxa). They contain a minor component of reworked Cretaceous material (generally less than 1%). However, compared to Dupuis et al. (2003), the number of specimens is rather low. Several levels are devoid of nannofossils, whereas others show selective preservation. Typical PETM-taxa are preserved in the interval 11.00–12.70 m (not described in this report), although in very low numbers (2 specimens of *Discoaster araneus* in interval 11.00–12.70 m, a few *Romboaster bitrifida* at 11.00 m, but no *Discoaster anartios* at all). From this it follows that the interval studied in detail here (2.75 m to 10.0 m) represents the uppermost Paleocene and provides insight into the paleoenvironmental setting just prior to the PETM.

Foraminiferal biostratigraphy

Planktic foraminifera are nearly absent in the upper Paleocene sediments. In all samples, the percentage of planktic specimens is well below 1%, with the exception of the phosphatic layer with an elevated percentage of 14%. The rare presence of *Morozovella velascoensis* indicates foraminiferal Zones P4 or P5. The associated calcareous nannofossil assemblage, indicative of NP9a, suggests that the studied interval only comprises the top part of Subzone P4c or Zone P5 (sensu Berggren and Pearson, 2005; which is equivalent to the lower part of Zone P5

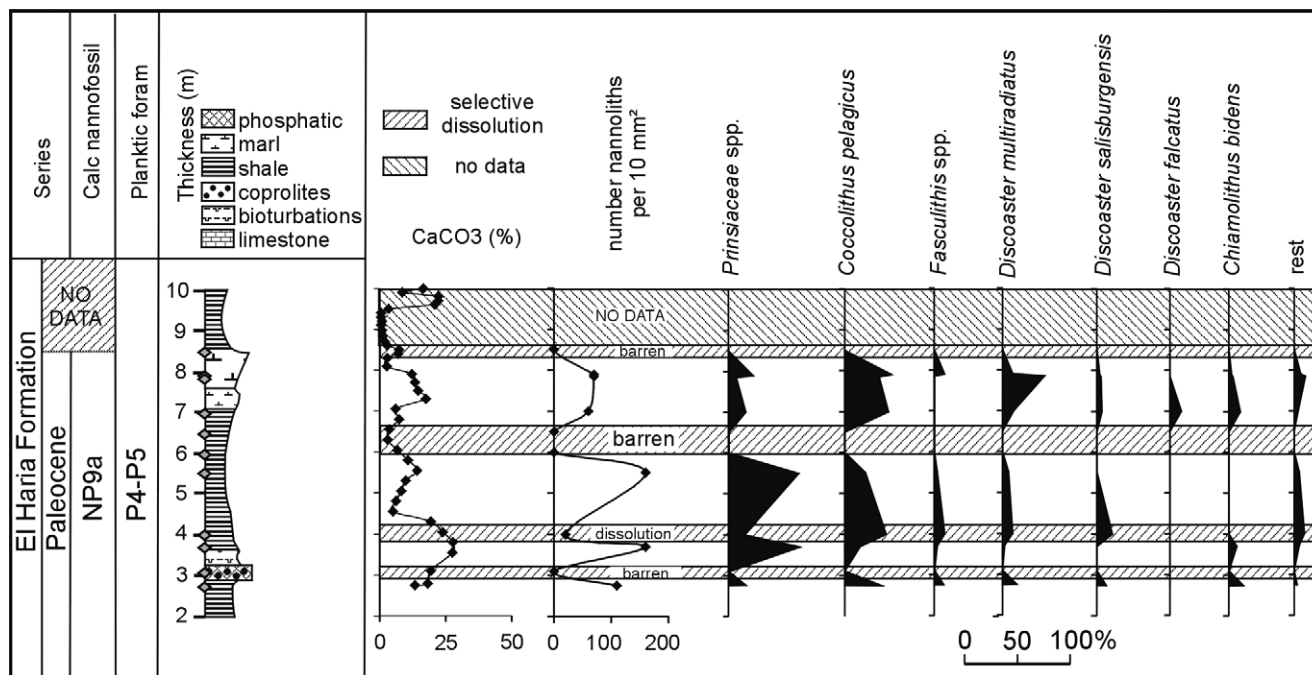


FIGURE 3 | Quantitative nanofossil data of the uppermost Paleocene at Sidi Nasseur. The quantitative data show that the distribution of nanofossils is strongly influenced by post-mortem dissolution processes (hatched intervals) with lower absolute numbers of nanoliths.

sensu Berggren et al., 1995). The large (up to 5 mm) benthic foraminifera *Fron dicularia phosphatica* has an almost continuous distribution. The highest occurrence of *F. phosphatica* is at 10.0 m. This distribution pattern is identical to the one observed at Gebel Duwi in Egypt, where the highest occurrence of *Fron dicularia phosphatica* enables a field identification of the P/E boundary (Speijer et al., 1996).

Ostracode record

Ostracodes occur almost continuously in the uppermost Paleocene part of the Sidi Nasseur section (Fig. 4). A total of 17 species have been retrieved, in a generally good preservation state and variable abundance. Twelve species are already known from previous records. Of these, *Aegyptiana duwiensis*, *Reymenticosta ben soni*, *Paracosta kefensis* (morphotype A: Bassiouni and Luger, 1990), *Paracosta* aff. *mokattamensis* and *Buntonia* sp. 3 (Donze et al., 1982) are known to be restricted to the upper Paleocene in Tunisia and Egypt (Donze et al., 1982; Bassiouni and Luger, 1990; Morsi and Speijer, 2003). Other known taxa include *Protobuntonia nakkadii* which appeared in the Maastrichtian, *Paracypris* sp. B (Esker 1968) which first appeared in the Danian. Both taxa have not been recorded higher than in the upper Paleocene. Furthermore, *Cytherella farafraensis*, *Paracypris jonesi*, *Cytheropteron lugeri*, *Parakrithe crolifa*, *Reticulina lamellata*, *Reticulina proteros* and *Reticulina sangalka mensis* are known to extend higher up into the lower

Eocene (e.g., Bassiouni and Luger, 1990; Morsi, 1999; Bassiouni and Morsi, 2000). The known distribution patterns of these ostracode taxa are well compatible with an uppermost Paleocene age for these deposits.

FORAMINIFERAL δ¹⁸O AND δ¹³C RECORDS

Foraminiferal preservation

Stable isotopic studies (C, O) on foraminifera from uplifted lower Paleogene sections (e.g., in Israel, Spain, Italy, Tunisia) are generally hampered by diagenetic problems (Schmitz et al., 1996). In order to reconstruct reliable carbon and oxygen records, an assessment of the preservation of foraminiferal calcite is needed. Careful examination of microstructures using both optical microscopy and electron microscopy can support the detection of diagenetic alteration, but results are not full proof (Marshall, 1992). Visual inspection of benthic foraminiferal tests under an optical binocular microscope showed that the majority of larger species (*Fron dicularia*, *Pyramidulina* and *Lenticulina*) is well preserved and unaltered (Fig. 5). Most foraminiferal species lack calcite overgrowths on the exterior wall, but usually contain infillings of secondary calcite. A scanning electron microscope investigation confirmed that in most specimens, only the interior void is filled by diagenetic calcite. The infillings in the tests of *Lenticulina* spp., other small calcareous benthic foraminifera and planktic foraminifera

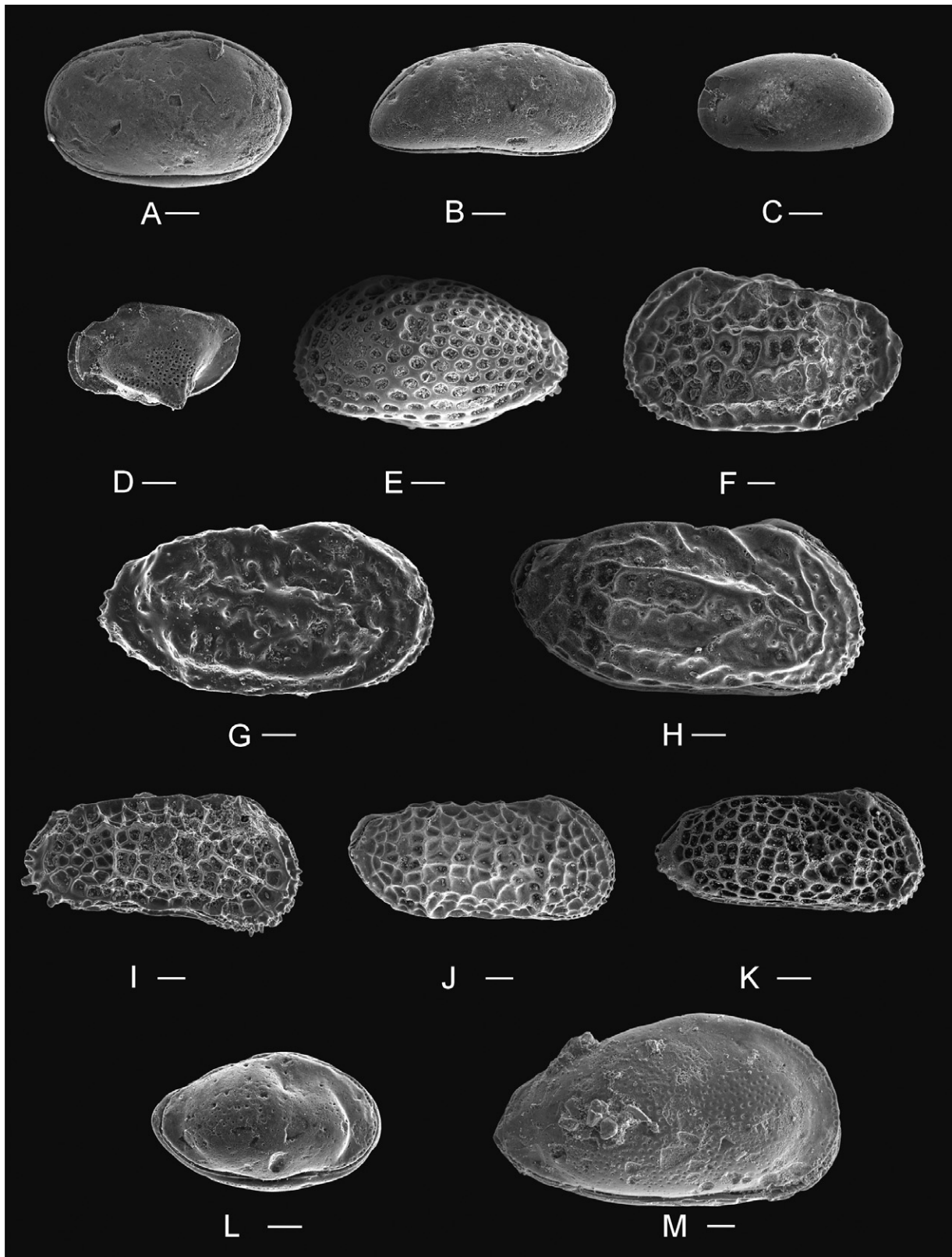


FIGURE 4 | Sample origin of the specimens is given between square brackets. All scale-bars represent 100 μm . A) *Cytherella farafraensis* [NAS 3.70 m]. B) *Paracypris* sp. B, Esker, 1968 [NAS 3.70 m]. C) *Parakrithe crolifa* [NAS'06 0.5; ~3.8 m]. D) *Cytheropteron lugeri* [NAS 3.70 m]. E) *Aegyptiana duwiensis* [NAS 7.90 m]. F) *Paracosta kefensis* [NAS 7.90 m]. G) *Paracosta* aff. *mokattamensis* [NAS 3.70 m]. H) *Reymenticosta bensoni* [NAS 7.90 m]. I) *Reticulina lamellata* [NAS 3.70 m]. J) *Reticulina proteros* [NAS 3.70 m]. K) *Reticulina sangalkamensis* [NAS 3.70 m]. L) *Buntonia* sp. 3, Donze et al., 1982 [NAS 3.70 m]. M) *Protabuntonia nakkadii* [NAS 3.30 m].

were impossible to remove. As a consequence, the tests of *Fron dicularia phosphatica* and *Pyramidulina latejugata* were analysed in this study. The thick-walled *P. latejugata* does not seem to be affected by diagenetic alteration and well-preserved specimens with original shell structure occur in many levels. In samples from the lower part of the section, well-preserved specimens of *Fron dicularia phosphatica* can be found with original internal structures and no or only minor infillings of the inner voids. In contrast, a wide variety of different states of preservation characterize *Fron dicularia* tests from other parts of the section. *Fron dicularia* specimens sometimes show intense secondary calcite overgrowths on the exterior surface wall. These overgrowths made it impossible to compose a reliable complete isotopic record based upon *Fron dicularia* specimens. Therefore thick-shelled *Pyramidulina latejugata* specimens were chosen to construct a single specimen foraminiferal isotopic record, because the tests are only filled by diagenetic calcite, easily removable by crushing the tests and picking the clean shell fragments.

Measurements on *Pyramidulina latejugata* and *Fron dicularia phosphatica* from the same intervals generally give similar results. A variety of different post-depositional processes may have affected the isotopic records and seemingly well-preserved *Pyramidulina* specimens occur in the same levels with less well-preserved *Fron dicularia phosphatica* specimens with secondary calcite overgrowth on the tests (Fig. 5). Significant alteration of the tests seems unlikely, given the pristine nature of the wall texture, the stability of the isotopic record and the large offsets between the isotopic values of the infillings – especially in oxygen isotopes – and the test walls.

Foraminiferal $\delta^{13}\text{C}$ and $\delta^{18}\text{O}$ records

The foraminiferal $\delta^{13}\text{C}$ record (*P. latejugata*, Fig. 6, Table 1) is fairly stable, with individual values varying between -1.3 and 0.7‰ . The variation of replicate measurements on the foraminiferal tests from the same horizon is relatively low (average 0.6‰). The few measurements (2.75 m to 3.7 m) on well preserved *Fron dicularia phosphatica* specimens gave comparable $\delta^{13}\text{C}$ values between -1.1 to -0.2‰ that fall within the scatter zone of *P. latejugata* $\delta^{13}\text{C}$ values, indicating minimal non-equilibrium fractionation caused by vital effects and similar microhabitat preferences. $\delta^{13}\text{C}$ values of the calcite infillings reveal a large variation between -6.5 to -0.4‰ and are mostly lower than -3‰ . Two measurements on infillings, however, fall within the scatter zone of multiple *P. latejugata* measurements.

The foraminiferal $\delta^{18}\text{O}$ values (Fig. 6) are between -2.9‰ (measured in the lowermost calcareous phosphatic bed at 2.80 m and 3.10 m) and -1.4‰ (8.5 m). This shows

a trend towards more positive $\delta^{18}\text{O}$ values. Only a minor scatter is measured (average 0.4‰) in samples with multiple isotopic analyses. The few measurements (2.75 m to 3.7 m) on well-preserved *Fron dicularia phosphatica* specimens have comparable $\delta^{18}\text{O}$ values between -2.6 and -2.0‰ . $\delta^{18}\text{O}$ values of the calcite infillings reveal a larger variation between -4.9 and -2.4‰ . The $\delta^{18}\text{O}$ values of the infillings are always lower than the values of the cleaned *Pyramidulina latejugata* specimens.

FAUNAL PATTERNS

Benthic foraminifera

General faunal composition

Calcareous benthic foraminifera were identified to species or genus level (Fig. 7 and Table 2). The latter applies to *Lenticulina* spp., other nodosariids and most agglutinated taxa. The preservation of the non-calcareous agglutinated foraminifera taxa is poor, limiting the taxonomic assignments. Therefore rare *Trochammina* spp. are lumped together with *Haplophragmoides* spp. (probably *Haplophragmoides excavata/walteri*). Throughout the section, non-calcareous agglutinated foraminifera are a major component of the assemblage, occasionally up to 100% and with major fluctuations. Therefore relative numbers and distribution patterns of calcareous and non-calcareous agglutinated foraminiferal groups are calculated and discussed separately (Fig. 8).

The benthic foraminiferal assemblages of the middle fraction (125–630 μm) consist of numerous small calcareous benthic foraminifera. The assemblages are moderately diverse (between 5 and 20 taxa per sample with an average of 15 taxa per count of 200–300 specimens per sample), mostly dominated by a few species. The three most common taxa, *Lenticulina* spp., *Anomalinoidea midwayensis* and *Bulimina* spp. (*Bulimina ovata/quadrata* and *Bulimina* gr. *trigonalis*), control most changes in the foraminiferal frequency patterns. Species like *Anomalinoidea umboniferus*, *Cibicidoides praecursoria*, *Valvulineria scrobiculata* and *Neoepionides elevatus* occur with maximum frequencies of 15%. *Stainforthia* spp. and less common *Anomalinoidea*, *Cibicidoides* and *Gyroidinoides* species constitute the remaining part of the assemblages (Fig. 8). The uppermost Paleocene calcareous benthic assemblage at Sidi Nasseur is also characterized by the common occurrence of large benthic foraminifera such as *Fron dicularia phosphatica* and *Pyramidulina* spp. in the $>630 \mu\text{m}$ fraction.

The abundance of *Lenticulina* spp. gradually decreases with oscillations from 64% (2.75 m) to 20% (7 m).

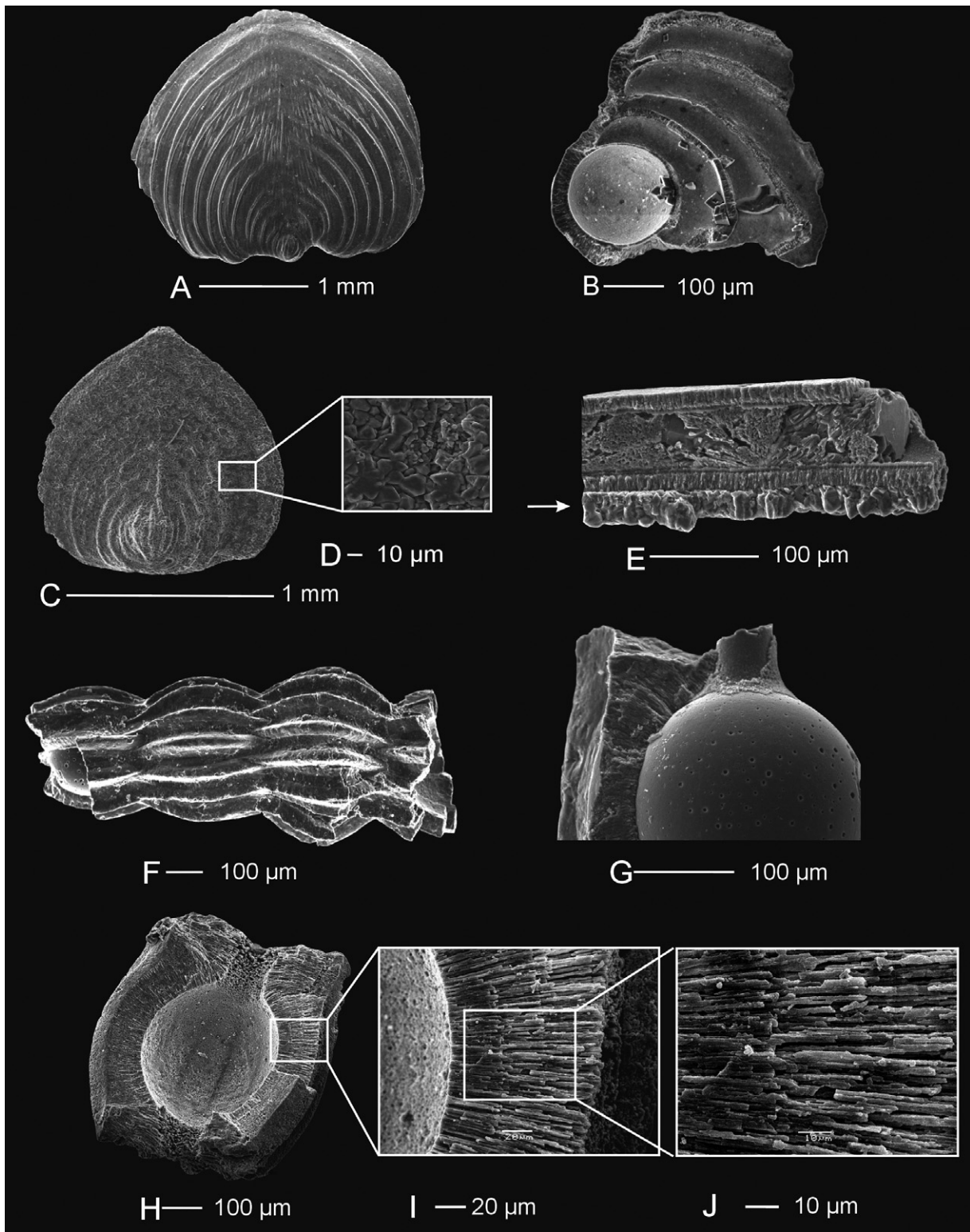


FIGURE 5 | Preservation of microfossils for stable isotope measurements. Sample origin of the specimens is given between square brackets. A) *Frondicularia phosphatica*, good preservation of the outer test wall [NAS 2.75 m]. B) *Frondicularia phosphatica*, good preservation of internal structures and no infillings of the inner voids [NAS 2.75 m]. C) *Frondicularia phosphatica*, poor preservation of the outer test wall due to overgrowth by secondary calcite [NAS 5.50 m]. D) Magnification of the calcite overgrowths of C. E) Crushed *Frondicularia phosphatica* with an infilling of the interior voids; arrow indicates the massive secondary calcite overgrowth on one side of the test [NAS 5.50 m]. F) *Pyramidulina latejugata*, good preservation of the outer test [NAS 2.75 m]. G) Crushed *Pyramidulina latejugata* with a complete infilling of the chamber by secondary calcite. These infillings are relatively easy to remove [NAS 2.75 m]. H) Excellently preserved *Pyramidulina latejugata* with details of original shell texture [NAS 8.50 m]. I) and J) are magnifications of the preserved microstructures of H.

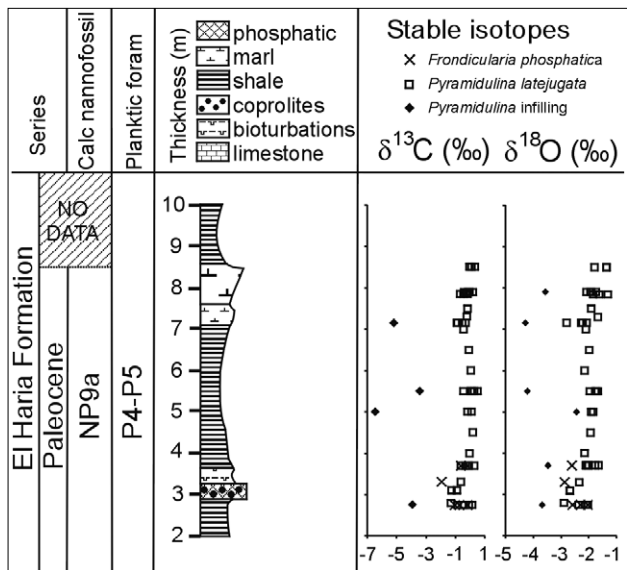


FIGURE 6 | Isotope results of the studied locality.

From 7.3 m to 10 m onwards, *Lenticulina* spp. values generally range between 10-20%. *Anomalinoidea midwayensis* is the most common and dominant species (min. 16.5%, max. 78% and mean 42%). Most samples with lowered abundance of *A. midwayensis* usually contain higher numbers of *Bulimina* and *Stainforthia* spp. The buliminid group (*Bulimina* spp. and *Stainforthia* spp.) is more important (10 to 60%) at certain levels, compared to most levels (<2.5%). The last common occurrences of several important Paleocene species in this section (*Lenticulina* spp., *A. midwayensis*, *A. umboniferus*, *Pyramidulina* spp., *F. phosphatica*) occur at 10 m.

Non-calcareous agglutinated foraminifera, composed of silicilastic and phosphatic material, are sometimes very frequent. The unavoidable lumping of non-calcareous taxa does not allow any insight into diversity patterns. Taxa are primarily distinguished from each other by large differences in overall morphology or wall composition. The most common and dominant group consists of finely cemented agglutinated *Haplophragmoides* spp. *Ammobaculites* spp. (probably *Ammobaculites expansus* and *Ammobaculites midwayensis*) are the other major components of the Paleocene assemblage. These non-calcareous agglutinated taxa incorporated phosphatic grains in their tests and are easily distinguishable from the *Haplophragmoides* group.

Foraminiferal numbers

Benthic foraminiferal numbers of calcareous taxa (Fig. 9) display large and rapid fluctuations throughout the section. Low numbers range between 0 and 100 speci-

TABLE 1 | Foraminiferal δ13C and δ18O record based upon single specimens of thick-shelled *Pyramidulina latejugata* and *Frondicularia phosphatica* specimens. (δ13C and δ18O are expressed as δ V-PDB).

Sample (m)	Species	δ13C (‰)	δ18O (‰)
2.75	<i>Frondicularia phosphatica</i>	-0.717	-2.571
2.75	<i>Frondicularia phosphatica</i>	-0.156	-2.024
2.75	<i>Frondicularia phosphatica</i>	-1.049	-2.285
3.3	<i>Frondicularia phosphatica</i>	-1.925	-2.863
3.7	<i>Frondicularia phosphatica</i>	-0.608	-2.595
2.75	<i>Nodosaria latejugata</i>	0.092	-2.241
2.75	<i>Nodosaria latejugata</i>	-0.801	-2.008
2.75	<i>Nodosaria latejugata</i>	-0.091	-2.367
2.75	<i>Nodosaria latejugata</i>	-0.847	-2.049
2.75	<i>Nodosaria latejugata</i>	-0.452	-2.039
2.8	<i>Nodosaria latejugata</i>	-1.283	-2.889
3.1	<i>Nodosaria latejugata</i>	-0.92	-2.684
3.1	<i>Nodosaria latejugata</i>	-1.259	-2.684
3.3	<i>Nodosaria latejugata</i>	-0.614	-2.333
3.7	<i>Nodosaria latejugata</i>	0.255	-2.01
3.7	<i>Nodosaria latejugata</i>	-0.127	-1.775
3.7	<i>Nodosaria latejugata</i>	-0.299	-2.05
3.7	<i>Nodosaria latejugata</i>	-0.626	-2.099
3.7	<i>Nodosaria latejugata</i>	-0.091	-1.651
4	<i>Nodosaria latejugata</i>	-0.051	-2.143
4.5	<i>Nodosaria latejugata</i>	0.187	-1.941
5	<i>Nodosaria latejugata</i>	-0.182	-1.922
5	<i>Nodosaria latejugata</i>	0.101	-1.834
5.5	<i>Nodosaria latejugata</i>	0.155	-1.969
5.5	<i>Nodosaria latejugata</i>	0.269	-1.718
5.5	<i>Nodosaria latejugata</i>	0.057	-1.774
5.5	<i>Nodosaria latejugata</i>	-0.046	-1.713
5.5	<i>Nodosaria latejugata</i>	-0.484	-1.933
5.5	<i>Nodosaria latejugata</i>	0.511	-1.668
6	<i>Nodosaria latejugata</i>	0.05	-2.141
6.5	<i>Nodosaria latejugata</i>	-0.091	-1.982
7	<i>Nodosaria latejugata</i>	-0.465	-2.101
7.15	<i>Nodosaria latejugata</i>	-0.532	-2.265
7.15	<i>Nodosaria latejugata</i>	-0.875	-2.787
7.15	<i>Nodosaria latejugata</i>	-0.882	-2.213
7.15	<i>Nodosaria latejugata</i>	-0.327	-2.07
7.3	<i>Nodosaria latejugata</i>	-0.235	-1.676
7.5	<i>Nodosaria latejugata</i>	-0.184	-1.904
7.85	<i>Nodosaria latejugata</i>	-0.667	-1.848
7.85	<i>Nodosaria latejugata</i>	-0.186	-1.312
7.85	<i>Nodosaria latejugata</i>	-0.433	-1.618
7.9	<i>Nodosaria latejugata</i>	-0.042	-1.753
7.9	<i>Nodosaria latejugata</i>	-0.384	-1.912
7.9	<i>Nodosaria latejugata</i>	0.19	-2.088
7.9	<i>Nodosaria latejugata</i>	-0.098	-1.931
8.5	<i>Nodosaria latejugata</i>	0.11	-1.352
8.5	<i>Nodosaria latejugata</i>	-0.039	-1.364
8.5	<i>Nodosaria latejugata</i>	0.328	-1.793
2.75	infilling of <i>Nodosaria</i>	-4.07	-3.678
3.7	infilling of <i>Nodosaria</i>	-0.378	-3.47
5	infilling of <i>Nodosaria</i>	-6.475	-2.428
5.5	infilling of <i>Nodosaria</i>	-3.441	-4.213
7.15	infilling of <i>Nodosaria</i>	-5.203	-4.285
7.9	infilling of <i>Nodosaria</i>	-0.406	-3.561

mens per gram sediment, mean values are ~225 specimens/g and multiple peaks >500 specimens/g. The buliminid group is frequently associated with higher foraminiferal numbers. The buliminids make up ~10 to 58% of the total calcareous assemblage in these intervals

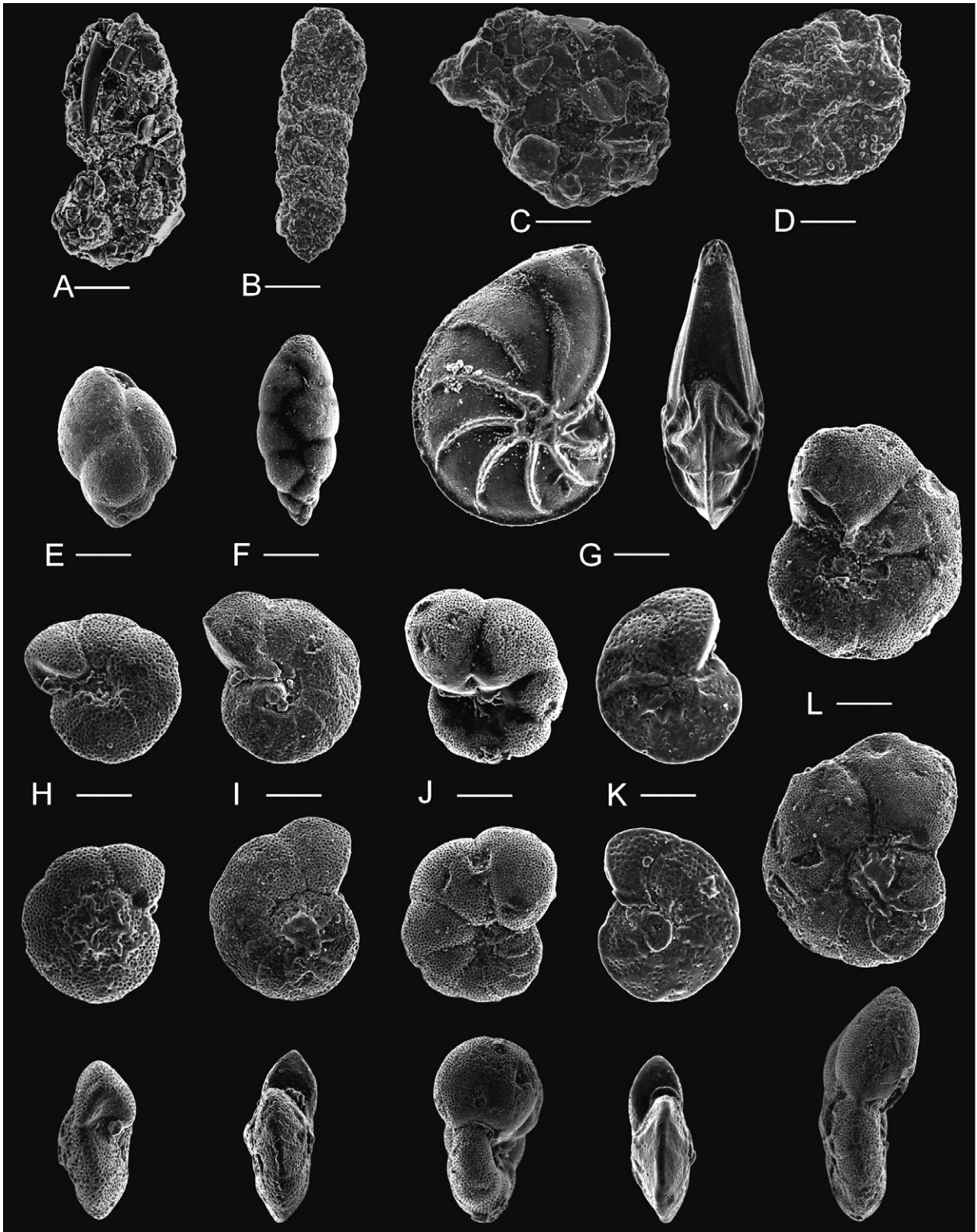


FIGURE 7 | Sample origin of the specimens is given between square brackets. All scale-bars represent 100 μ m. A) *Ammobaculites midwayensis* [NAS'06 6.7; ~10 m]. B) *Spiroplectammina mexiaensis* [NAS 7 m]. C) *Ammobaculites expansus* [NAS 9.5 m]. D) *Haplophragmoides excavata/walteri* [NAS 4.50 m]. E) *Bulimina* gr. *ovata/quadrata* [NAS 7.85 m]. F) *Bulimina* gr. *trigonalis* [NAS'06 6.5; ~9.80 m]. G) *Lenticulina pseudomamilligera* [NAS'06 4; ~7.3 m]. H) *Neoepionides elevatus* [NAS 7.90 m]. I) *Anomalinoidea midwayensis* [NAS 7.50 m]. J) *Valvulineria scrobiculata* [NAS 3.70 m]. K) *Cibicoides praecursoria* [NAS'06 4; ~7.30 m]. L) *Anomalinoidea umboniferus* [NAS 3.70 m].

with higher foraminiferal numbers, in contrast to other samples where they constitute <2.5%. Foraminiferal numbers of non-calcareous taxa are more stable (~100 specimens/g) with multiple peaks (>260 specimens/g). Lower foraminiferal numbers of calcareous benthic foraminifera (<100/g) correspond to intervals with very high abundances of non-calcareous agglutinated foraminifera (up to 100%). In contrast, absolute numbers of non-calcareous agglutinated foraminifera do not follow the fluctuations in relative abundances of non-calcareous agglutinated foraminifera. Peaks in non-calcareous agglutinated foraminiferal numbers usually correspond with higher numbers of calcareous benthic foraminifera per gram.

DISCUSSION

Biotratigraphy

Sediments of the Sidi Nasseur section contain the typical latest Paleocene nannofossil taxa of the top of NP9a. The last common occurrences of several common Paleocene taxa (*Lenticulina* spp., *A. midwayensis*, *A. umboniferus*, *Pyramidulina* spp. and *Fronidularia phosphatica*) mark an important turnover between 10.0 m and 10.1 m. *Pyramidulina* and *Fronidularia* species do not reappear above this horizon. In deep-sea to outer neritic deposits, the extinction of *Gavelinella beccariiformis*, *Angulogavelinella avnimelechi* and other taxa marks the P/E boundary (Tjalsma and Lohmann, 1983; Speijer et al., 1996; Thomas, 1998). Our observations from Sidi Nasseur combined with those from Gebel Duwi in Egypt suggest that the extinction of *F. phosphatica* is an equally excellent stratigraphic marker –even in the field– for the P/E boundary in inner-middle neritic deposits of North Africa. However, Luger (1985) and Youssef (2003) observed *F. phosphatica* also in lower Eocene beds in Central Egypt. Assuming that the taxonomic identifications of this diagnostic species are correct, the disappearance of *F. phosphatica* at Sidi Nasseur and Gebel Duwi may only reflect local biofacial changes and not extinction.

The uppermost Paleocene stable isotopic signature of the southern Tethys

Stable isotope records (Fig. 10) have been established in upper Paleocene sections at Gebel Duwi (Egypt, paleodepth 75–100 m) and Gebel Aweina (Egypt, paleodepth 150–200 m). The upper Paleocene $\delta^{13}\text{C}$ values in both sections are between 0 and 1‰. A gradual negative change of ~1‰ is observed in the uppermost Paleocene part of the sections, starting about 5 to 10 m below the onset of the CIE (Schmitz et al., 1996; Charisi and Schmitz, 1998). At Gebel Aweina, $\delta^{13}\text{C}$ values in top 5

meters (NP9 and based upon *Pyramidulina latejugata*) are around 0‰. The $\delta^{18}\text{O}$ values vary around -2‰ (Charisi and Schmitz, 1998). In Gebel Duwi, the $\delta^{13}\text{C}$ values in top 5 meters (NP9 and based upon *Fronidularia* spp.) vary between -1 and 0‰, $\delta^{18}\text{O}$ values are around -2‰ (Schmitz et al., 1996). Although the isotope records from Sidi Nasseur (Tunisia, *Pyramidulina latejugata*) and Gebel Duwi (Egypt, *Fronidularia* spp.) are compiled using different species, they are comparable with only minimal interspecific differences. The established isotope record (especially $\delta^{13}\text{C}$) of the uppermost Paleocene sediments at Sidi Nasseur resembles the Tethyan values of the uppermost Paleocene at Gebel Duwi and Gebel Aweina (Fig. 10).

Taphonomy and paleoproductivity

Foraminiferal numbers depend on three factors: test production, dilution by other sedimentary particles and post-depositional dissolution of calcareous components. Dissolution effects cause an underestimation of the foraminiferal numbers. The combination of high percentages of non-calcareous agglutinated foraminifera and low absolute numbers of calcareous benthic foraminifera and planktic foraminifera are often regarded as an indicator of strong taphonomic alteration (Murray, 1991). The lack of elevated absolute numbers of non-calcareous agglutinated foraminifera per gram sediment indicates that the high relative numbers of this group are caused by the near absence of calcareous foraminifera, rather than by a bloom of agglutinated foraminifera. The inferred dissolution intervals (4.05–4.3 m, 6.3 m, 8.1 m, and 8.7–9.4 m) are recognized by low absolute numbers of calcareous benthic foraminifera per gram and high percentages of non-calcareous agglutinated taxa (Fig. 9). The uppermost interval is almost entirely decalcified. It is most likely that agglutinated assemblages in the fossil record are primarily the product of post-mortem dissolution processes leaving the residue dominated by agglutinated forms, rather than characteristic of a living benthic assemblage with only agglutinated taxa (Murray, 1991). The quantitative nannofossil data also show that their distribution is taphonomically controlled (Fig. 3). The family Prinsiacae, which is essentially made up of tiny forms, dominates (66% of the association) in samples with the highest concentration in nannofossils. When concentrations decrease, because of more severe carbonate dissolution, the more robust forms, such as *Discoaster multiradiatus*, *Coccolithus pelagicus* and *Fasciculithus* spp. increase in relative abundance.

The effect of dilution by other sedimentary particles is not well constrained at Sidi Nasseur, but is thought to play an important factor too. Higher amounts of benthic foraminifera per gram can be indicative of condensation

TABLE 2 | Benthic foraminiferal frequency data of the most common taxa (>5% in at least one sample). Note that calcareous benthic foraminifera

Sample (m)	NAS	NAS	NAS'06	NAS	NAS'06	NAS	NAS	NAS	NAS	NAS
2.75	2.80	3.55	3.70	4.05	4.50	5.00	5.50	6.00	6.50	
<i>Spiroplectammia spectabilis</i>	0.0	0.0	0.0	0.0	0.8	0.0	0.7	0.0	1.6	3.0
<i>Ammobaculites</i> group	0.0	0.0	19.8	10.3	10.2	7.6	1.3	0.4	4.9	3.0
<i>Haplophragmoides</i> spp.	99.5	100.0	80.2	86.2	88.5	84.0	96.0	97.8	92.6	93.0
rest	0.5	0.0	0.0	3.4	0.5	8.4	2.0	1.8	0.8	1.1
number agBF	209	40	86	29	392	131	149	277	122	270
<i>Bulimina ovata/quadrata</i>	0.6	0.0	0.6	6.5	0.0	0.5	0.9	5.8	0.0	0.0
<i>Bulimina</i> gr. <i>trigonalis</i>	0.0	0.0	0.0	6.0	0.0	0.0	0.0	6.2	0.0	0.0
<i>Bulimina kugleri</i>	0.0	0.0	1.6	2.8	0.0	0.5	0.5	6.7	0.0	0.0
<i>Stainforthia</i> spp.	0.6	0.9	0.0	0.5	0.0	0.0	0.0	0.0	0.0	0.0
<i>Lenticulina</i> spp.	64.2	37.1	13.8	19.0	35.1	24.8	44.7	23.1	36.3	23.3
<i>Alabamina midwayensis</i>	1.7	6.0	5.0	5.6	4.5	2.9	0.0	2.7	0.6	0.0
<i>Neceponides elevatus</i>	3.4	2.6	4.7	3.2	11.9	4.4	14.3	8.0	3.6	2.3
<i>Anomalinoidea umbonifera</i>	0.0	0.0	5.7	10.2	0.7	0.0	0.0	1.8	0.0	0.3
<i>Anomalinoidea midwayensis</i>	17.6	16.4	44.7	29.2	31.3	60.2	30.9	24.9	53.6	72.2
<i>Anomalinoidea</i> spp.	4.0	0.0	7.2	0.5	2.2	0.0	0.0	0.0	0.0	0.0
<i>Cibicoides praecursoria</i>	0.6	14.7	5.0	4.6	5.2	1.0	0.5	0.0	0.0	0.0
<i>Cibicoides</i> spp.	2.8	2.6	1.9	0.9	0.7	0.0	0.0	0.0	0.0	0.0
<i>Valvulineria scrobiculata</i>	0.6	4.3	2.2	4.2	3.7	2.4	5.5	12.9	0.0	0.0
rest	4.0	15.5	7.5	6.9	4.5	3.4	2.8	8.0	6.0	1.9
number calcBF	176	116	318	216	134	206	217	225	168	309

and/or winnowing of the clay fraction and not for elevated test production. Most fluctuations in foraminiferal numbers probably result from the combination of these post-depositional taphonomic effects and variations in calcareous test production seem not determinable in this specific situation. Studies on recent highly productive shallow water environments indicate that taphonomic processes may result in a rapid decline in absolute numbers of calcareous tests. Many calcareous species live in coastal settings but there is a significant taphonomic loss in the transition from living to fossil assemblages with an overall increase in relative abundance of agglutinated foraminifera (Berkely et al., 2007). These taphonomic features are recognized in shallow subtidal sediments (e.g., Oslo Fjord and Long Island Sound), intertidal sediments (e.g., northern Gulf of Mexico) and marsh sediments (Murray and Alve, 1999b). Carbonate dissolution within the substrate is linked with the occurrence of organic material in the taphonomically active zone where oxidization of organic material is possible. The consumption of organic material leads to higher levels of dissolved CO₂ in pore water (Murray and Alve, 1999a/b; Berkely et al., 2007). This in turn leads to the assumption that calcareous test preservation is closely linked with organic productivity. In the Sidi Nasseur section, samples with the lowest calcareous foraminiferal numbers might in fact reflect the intervals with the highest productivity, but with sufficient oxygen to degrade the organic material deposited in the sediments. The absence of organic-walled dinocysts in the studied samples (Van Simaëys, pers. comm. 2005), contrasting with their high-abundance lower in the Paleocene succession and in other

localities exposing the El Haria Fm (Guasti et al., 2006) suggests that the organic component of the NAS sediments is indeed strongly degraded.

Paleobathymetry

Planktic/benthic (P/B) ratio is expressed as the percentage of planktic specimens in the total foraminiferal assemblage. The P/B ratio is often used to estimate the paleobathymetric evolution of a basin (Van der Zwaan et al., 1990). Provided that normal marine conditions occurred at the time of deposition and dissolution has not affected the foraminiferal assemblage, the P/B ratio may provide a good indication of paleodepth. In the Sidi Nasseur section, planktic foraminifera are nearly absent (max. 20 specimens/g) with P/B ratios well below 1% in most samples. These low numbers persist in intervals which are considered hardly affected by post-mortem dissolution. In comparison with data on modern continental margins, planktic percentages lower than 4% correspond to water depths less than 30 m in the Gulf of Mexico and less than 70 m in the semi-enclosed Adriatic Sea (Van der Zwaan et al., 1990). Consequently, our data point to deposition in a restricted shallow basin with connections to the open marine Tethys as can be judged from the common presence of calcareous nannofossils. The upper Paleocene part of the El Kef section, 50 km to the north, yields P/B ratios <10% and is considered to represent an inner neritic (Kouwenhoven et al., 1997; Guasti et al., 2005). Since El Kef was located more offshore from the Kasserine high than the Kalaat Senan area (Guasti et al., 2006), an even shallower inner neritic to coastal deposition at Sidi Nasseur is plausible.

(calcBF) and non-calcareous agglutinated benthic foraminifera (agBF) are treated separately with different splits.

NAS	NAS'06	NAS	NAS'06	NAS	NAS	NAS'06	NAS'06	NAS'06	NAS'06	NAS'06	NAS'06	NAS'06	NAS'06
7.00	7.30	7.50	7.70	7.85	7.90	8.50	9.00	9.40	9.60	9.70	9.80	9.90	10.00
8.1	3.3	0.9	1.9	2.2	0.0	0.0	1.8	0.3	5.6	0.0	0.0	4.5	0.0
0.0	0.0	8.4	0.0	0.9	0.0	15.8	8.1	2.2	68.1	34.5	12.8	17.9	32.5
89.9	95.0	88.8	95.5	96.0	96.1	84.2	89.5	94.7	26.4	62.1	87.2	74.6	67.5
2.0	1.7	1.9	2.5	0.9	3.9	0.0	0.6	2.8	0.0	3.4	0.0	3.0	0.0
148	181	107	157	226	51	19	332	356	72	29	47	67	77
0.0	13.9	16.9	18.9	0.9	36.2	0.0			8.8	11.0	13.7	7.5	6.5
0.4	8.0	3.5	7.2	0.0	13.5	0.0			2.9	6.2	5.6	4.3	2.0
0.0	1.2	4.5	0.6	0.0	3.7	0.0			0.0	0.0	1.5	0.0	0.2
0.4	8.3	3.5	4.3	0.5	4.9	0.0			0.8	0.7	1.2	1.2	2.5
19.7	11.4	17.9	15.8	28.8	11.0	13.8			18.7	10.3	9.6	12.7	14.5
0.0	0.0	0.0	0.0	0.0	0.0	0.0			0.0	0.0	0.0	0.0	0.2
9.2	3.4	4.0	6.6	11.0	6.7	3.4			6.7	3.4	3.8	5.5	5.6
3.8	2.8	4.5	2.3	0.0	1.8	0.7			4.3	3.4	3.1	0.0	0.0
57.3	36.7	23.9	26.6	43.8	14.1	77.8			44.3	52.2	48.3	58.0	54.1
3.3	2.2	6.0	2.0	3.7	1.2	0.0			0.0	1.4	0.2	0.0	2.0
0.0	2.2	2.5	1.1	0.5	1.2	0.0			0.0	0.0	0.2	0.4	0.0
0.0	0.3	0.0	0.0	0.0	0.0	0.0			0.8	3.8	5.6	6.1	3.6
3.8	2.5	8.0	6.3	7.3	3.1	2.0			6.4	1.0	2.6	1.4	4.0
2.1	7.1	5.0	8.3	3.7	2.5	2.4			6.4	6.5	4.5	2.9	4.7
239	324	201	349	219	163	297	0	0	375	291	604	510	551

Additional indications of paleodepth can be retrieved through analysis of paleobathymetrical ranges for individual benthic taxa and associations. Amongst the ostracodes, representatives of the genera *Aegyptiana*, *Paracosta*, *Reticulina* and *Reymenticosta* make up the major part of the ostracode fauna. These genera are typically trachyleberidid shelf genera possessing eye tubercles and dominating within the euphotic zone. Among these, *Reymenticosta bensoni* is the most abundant species. Through comparison with P/B ratios in southern Egypt, this species was assigned by Bassiouni and Luger (1990) to a middle to inner shelf setting.

Paleobathymetrical and paleoenvironmental distribution patterns are also established for benthic foraminifera. Figure 11 represents the composition of benthic foraminiferal associations of several upper Paleocene southern Tethyan sections, arranged along a depth gradient. Bou Dagher (1987) and also Aubert and Berggren described (1976) peculiar benthic associations dominated by *Stainforthia* spp., *Elphidiella prima* together with some other species such as *Nonionella insecta* or *Anomalinoidea umboniferus*. These forms are thought to typify a restricted hyposaline nearshore or lagoonal facies. According to a quantitative analysis by Saint-Marc and Berggren (1988 and based on the dataset of Aubert and Berggren, 1976), a near-shore Tunisian Paleocene benthic foraminiferal assemblage is composed of *A. umboniferus*, *B. gr. trigonalis* and *Neoeponides elevatus*. According to the same authors, an inner neritic assemblage is composed of *Lenticulina* spp., *Haplophragmoides* spp., *Fronidularia phosphatica* and *Bulimina quadrata/ovata*. We used the common taxa in the upper Paleocene sedi-

ments of the El Kef section as a reference for an inner neritic section (Kouwenhoven et al., 1997). Similar benthic foraminiferal assemblages as at Sidi Nasseur are also known from Egypt. In southeastern Egypt, Speijer et al. (1996) described in detail a middle neritic benthic foraminiferal assemblage from Gebel Duwi (Egypt) with paleodepths ranging between 75 and 100 m and P/B ratios >50%. Common taxa found in the upper Paleocene Dababiya (Egypt, Dababiya: Ernst et al., 2006) and Gebel Aweina (Egypt, Aweina: Speijer and Schmitz, 1998) sections function as a reference for an outer neritic Tethyan section with paleodepths between 150–200 m and P/B ratios ranging between 50–95%.

Stainforthia spp., *Lenticulina* spp. and *Valvulineria scrobiculata* have a wide bathymetric range. Species like *F. phosphatica* and large *Pyramidulina* spp. appear almost continuous in the Sidi Nasseur record and are indicators of open marine inner to middle neritic deposits in the southern Tethys (Aubert and Berggren, 1976; Saint-Marc, 1992; Speijer et al., 1996). High abundances of *Haplophragmoides* spp. are regarded as an indicator of shallow and restricted environments (Aubert and Berggren, 1976; Saint-Marc, 1992; Schnack, 2000). Furthermore, species typical for middle and outer neritic assemblages in the Southern Tethys occur only in minor proportions in the NAS section. The composition of the benthic foraminiferal association at Sidi Nasseur most resembles a near-shore (Djebel Mehiri Zebbeus: Aubert and Berggren, 1976) to inner neritic open marine environment (upper Paleocene at El Kef: Kouwenhoven et al., 1997). The foraminiferal association does not resemble a restricted hyposaline or lagoonal environment (Djebel

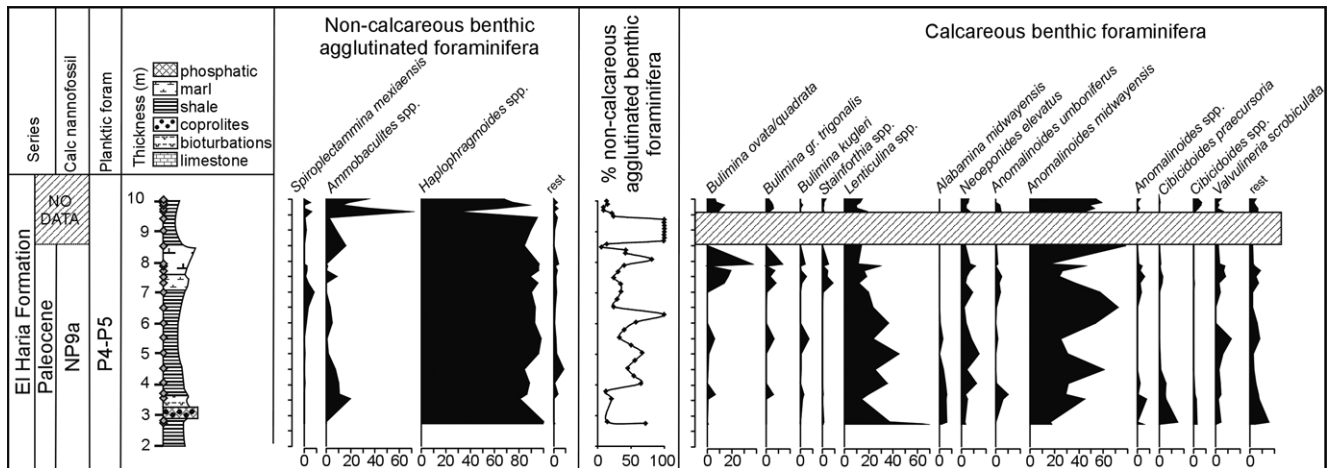


FIGURE 8 | Benthic foraminiferal frequency patterns of the most common taxa (>5% in at least one sample) of the uppermost Paleocene at Sidi Nasseur. Note that calcareous benthic foraminifera and non-calcareous agglutinated benthic foraminifera are treated separately and each group represents a 100% composition.

Chemsi and Djebel Hamadi: Aubert and Berggren, 1976 and Massanerh: Bou Dagher, 1987). The combination of characteristic open marine near-shore and inner neritic dwelling benthic foraminifera, combined with high dominance values (*A. midwayensis*, *Haplophragmoides* spp.) and the near absence of planktic foraminifera suggest that paleodepth was certainly less than 50 m (inner neritic) and probably even <20-30 m (coastal).

Berggren (1974, Rockall Bank in the North Atlantic Ocean) considered *Anomalinoidea midwayensis* and *Haplophragmoides* spp. as suggestive shallow water species for water depths <20 m. High dominances of *Anomalinoidea midwayensis* and *Ammobaculites* spp. are also regarded by Kellough (1965, Midway Group in northeast Texas) as indicators of intertidal to inner coastal settings. The decreasing abundance of *Lenticulina* spp. in the upper part of the section coincides with increasing abundances of *A. midwayensis* and *Ammobaculites* spp., which may suggest a shallowing from an inner neritic-coastal setting to a coastal setting during the latest Paleocene. A latest Paleocene sea-level fall just prior to the PETM was also observed at Gebel Duwi and may be eustatically controlled (Speijer and Morsi, 2002; Morsi and Speijer, 2003).

Paleotemperature and salinity

Oxygen isotope ratios are dependent on water temperature during the precipitation of shell calcite, the isotope composition of ambient sea water as well as non-equilibrium fractionation caused by vital effects (Murray, 1991). According to Charisi and Schmitz (1998), the carbon and oxygen isotope ratios of the costate nodosariid *Pyra-*

midulina do not deviate largely from equilibrium values. Assuming an ice-free world and no local influences, paleotemperatures can be calculated using the temperature equation given by Shackleton (1974).

$$T = 16.9 - 4.38 * (\delta_c - \delta_w) + 0.1 * (\delta_c - \delta_w)^2$$

T is the temperature in degree Celsius; δ_c the oxygen isotope ratio of foraminiferal calcite test in permil V-PDB and δ_w is the $\delta^{18}\text{O}$ of the seawater in permil V-SMOW. δ_w is assumed to be -1.0‰ in an ice-free world (Zachos et al., 1994 and Maslin and Swann, 2005). The calculated inner neritic bottom water temperatures for the NAS section range between 22°C (2.75 m) and 19°C (8.5 m). Zachos et al. (1994) reconstructed equator to high southern latitude sea surface temperatures for the late Paleocene. These reconstructions indicate that tropical sea surface temperatures were 20°C in the Pacific and 26°C in the Caribbean. Furthermore, tropical δ_w values are higher than the mean values (ice-free) due to enhanced evaporation and therefore can result in cooler apparent tropical temperatures (Zachos et al., 1994). Results from Pearson et al. (2001) on exceptionally well-preserved foraminifera shells, suggest that tropical sea surface temperatures were at least $28\text{--}32^\circ\text{C}$ during the Eocene. Average modern surface water temperatures of the Red Sea during summer range between 26°C in the north and 30°C in the south. All published paleotemperature estimates for the late Paleocene-Eocene and modern data indicate tropical sea surface temperatures higher than the calculated bottom water temperatures ($18\text{--}21^\circ\text{C}$) at Sidi Nasseur. In accordance to the very shallow marine setting (probably <20-30m), a significant vertical temperature gradient between sea surface temperatures and

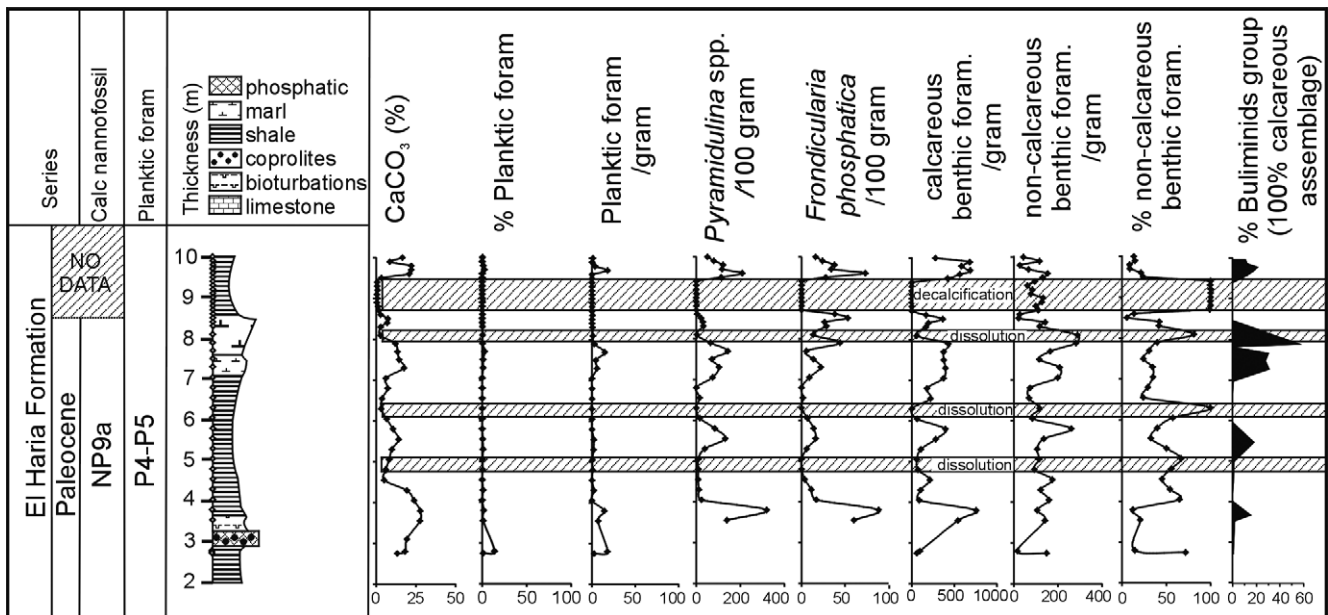


FIGURE 9 | General faunal characteristics indicating fluctuations in productivity levels and taphonomic effects like dissolution of the calcareous microfossil components. The hatched intervals correspond to levels with severe dissolution and an underestimation of the calcareous foraminiferal numbers.

bottom water temperatures is not likely at Sidi Nasseur. The calculated bottom water temperatures at Sidi Nasseur are too low for shallow tropical water during the latest Paleocene.

Kouwenhoven et al. (1997) argued that the inner-middle neritic (late Paleocene), highly eutrophic environment of El Kef (50 km to the north of Sidi Nasseur) may have been influenced by intensified upwelling of deeper waters. Observations from the Canary Current upwelling and observations along the southern coast of Australia suggest that a depth of 60 meter or more is needed to accommodate ocean upwelling dynamics when the winds blow parallel to the coast. Paleodepth estimations for the Sidi Nasseur section are too shallow (coastal setting, probably <20-30 m) to support the idea of colder water upwelling. Changes in the isotope composition of marginal marine and coastal waters are a more likely explanation. Evaporation leads to a higher δ_w than the considered -1.0‰ in an ice-free world. In order to obtain paleotemperatures higher than 25°C (bottom temperature), an oxygen isotope composition ($\delta_{w, \text{NAS}}$) higher than -0.4‰ has to be assumed for sea water at Sidi Nasseur. Neglecting any mixing of different water masses and freshwater input from the continent, the salinity/ $\delta^{18}\text{O}$ relationship is only dependent on the ratio of precipitation vs. evaporation (Rohling and Bigg, 1998). To calculate the salinity effect in a marginal basin, the salinity values of the Mediterranean are chosen for comparison. The eastern Mediterranean has a

well-established salinity (S) and $\delta^{18}\text{O}$ relationship (of $\delta^{18}\text{O} = 0.276814 * S - 9.07815$; Pierre et al., 1986). To explain the difference between the hypothetical $\delta_w -1.0\text{‰}$ (ice-free world) and the needed $\delta_{w, \text{NAS}}$; a salinity increase higher than 2 is needed, relative to mean salinity of the Paleocene oceans.

Mean $\delta^{18}\text{O}$ values are -2.2‰ at 2.75 m and -1.5‰ at 8.5 m. The 0.7‰ increase in the oxygen isotope values at Sidi Nasseur may reflect a paleoenvironmental change. The increasing dominance of *A. midwayensis* suggests a transition from an inner neritic-coastal setting to a shallower coastal setting during the latest Paleocene. This shallowing trend would involve higher bottom water temperatures and/or the formation of enclosed basins. By using the paleotemperature equations, the 0.7‰ increase corresponds to an unrealistic 3°C cooling of bottom waters during the latest Paleocene. On the other hand, the 0.7‰ increase in oxygen isotopes values translates into an extra 2.5-2.6 increase in salinity during the latest Paleocene at Sidi Nasseur as the result of increased evaporation in marginal marine water or increased evaporation in an enclosed basin.

Trophic and redox conditions

Benthic foraminiferal compositions are regulated by the interplay between organic flux, oxygen and competition. Environmental conditions with a high and unstable organic flux display low diverse benthic faunas with very

high dominance values (Murray, 1991). Organic flux (food supply) is important in regulating abundances, but is subordinate as soon as oxygen starts to be a limiting factor. In dysoxic conditions, the low bottom-water oxygen levels lead to the development of an impoverished stressed benthic fauna (Murray, 1991). This will certainly be the case in shallow water systems with muddy sedi-

ments (Van der Zwaan et al., 1999) like at Sidi Nasseur.

The Paleocene assemblage at Sidi Nasseur is dominated by *Lenticulina* spp., *Anomalinoidea midwayensis*, the buliminid group (*Bulimina* spp. and *Stainforthia* spp.) and the non-calcareous agglutinated *Haplophragmoides* spp. The very high dominances point to stressed conditions. *Lenticulina* makes up more than 40% of the assemblages in the lower part. Ernst et al. (2006) regarded *Lenticulina* as opportunistic oxygen-stress tolerant taxon. The co-occurrence of phosphate-rich sediments (at 3 m) with abundant *Lenticulina* indicates eutrophication of the environment which in turn may have led to a certain amount of oxygen deficiency at the seafloor and in the sediment. The buliminid group normally makes up <2.5% of the assemblages with maximum values of 60% in intervals with elevated benthic foraminiferal numbers. Modern *Bulimina* species usually occupy a shallow endobenthic microhabitat and may feed more on degraded organic carbon than most epibenthic taxa and are able to live in an oxygen deficient environment (Van der Zwaan et al., 1999). Only short intervals yield elevated numbers of *Bulimina* spp. and *Stainforthia* spp., coinciding with lower percentage of *A. midwayensis*. These short intervals with increased occurrences may represent periods of oxygen deficiency, affecting the occurrences of other calcareous benthic foraminifera. The continuous occurrence of *Valvulineria scrobiculata* is also indicative of a high organic flux, by analogy with neritic environments in Egypt and with modern *Valvulineria* species (Speijer, 1994). The occurrence of *Haplophragmoides* spp. also supports this idea, as this taxon is also regarded as tolerant to low-oxygen water conditions associated with organic-rich mud (Nagy et al., 1988; Saint-Marc and Berggren, 1988). Furthermore, these agglutinated foraminifera, composed of siliciclastic material hold together by organic cements, are not preserved under normal oxygen conditions due to microbial degradation of the organic cements (Berkeley et al., 2007). The high preservation potential of the non-calcareous agglutinated foraminifera in the Sidi Nasseur section, indicate lower oxygen levels.

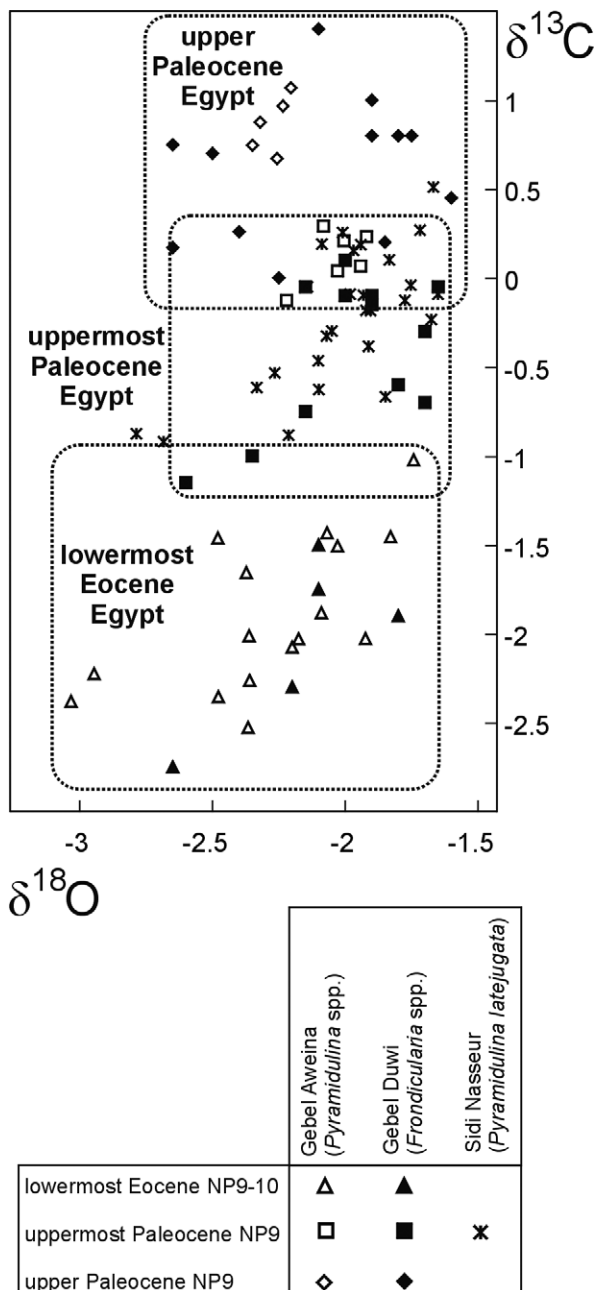


FIGURE 10 | Comparison of benthic carbon and oxygen isotopic records from upper Paleocene to lower Eocene sediments from southern Tethyan sections (Egypt, Gebel Aweina: Charisi and Schmitz, 1998; Egypt, Gebel Duwi: Schmitz et al., 1996).

The observed stress-fauna with high dominance values are the result of continuous eutrophic conditions with low oxygen concentrations during the latest Paleocene. Prolonged periods of severe oxygen deficiency are unlikely due to the absence of laminated sediments and the continuous presence of benthic fauna. The occasional interruptions by elevated percentages of the buliminid group resemble periods of possible elevated food supply and/or lower oxygen conditions at the seafloor. As discussed earlier, levels with lower calcareous foraminiferal numbers and higher abundances of non-calcareous agglutinated foraminifera might in fact reflect the intervals with high productivity under oxic conditions.

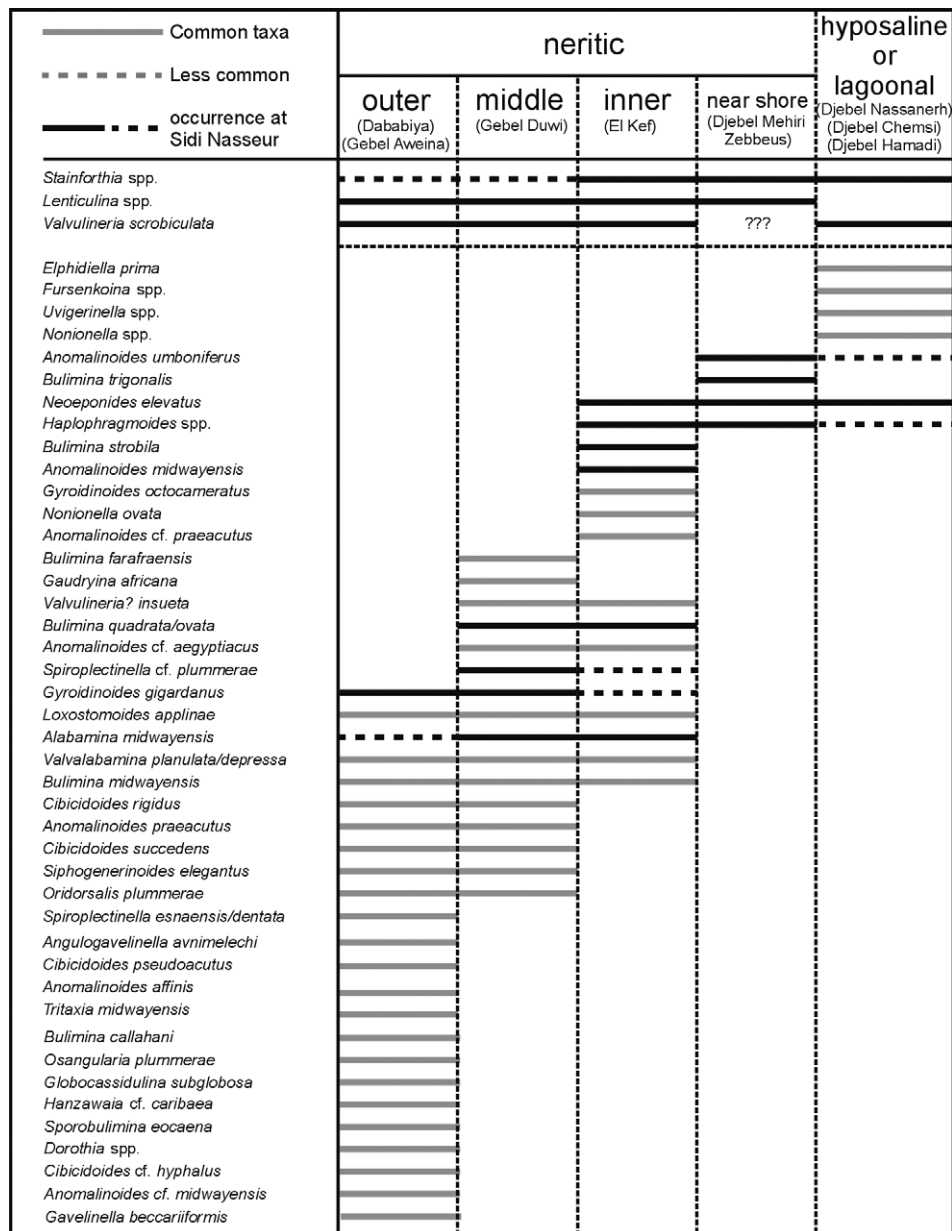


FIGURE 11 | Composition of benthic foraminiferal associations of several Paleocene southern Tethyan sections, arranged along a depth gradient (Dababiya, Egypt: Ernst et al., 2006; Gebel Aweina, Egypt: Speijer and Schmitz, 1998; Gebel Duwi, Egypt: Speijer et al., 1996; El Kef, Tunisia: Kouwenhoven et al., 1997; Djebel Mehiri Zebbeus, Tunisia: Aubert and Berggren, 1997; Massanerh, Tunisia: Bou Dagher, 1987; Djebel Chemsii and Djebel Hamadi, Tunisia: Aubert and Berggren, 1976).

CONCLUSIONS

The composition of the calcareous nannofossil association places the studied part of the Sidi Nasseur section in the uppermost Paleocene (top of nannofossil zone NP9a). The disappearance of the large and characteristic benthic foraminiferal species *Fronidicularia phosphatica* at 10 m promotes its potential as an excellent field marker for the Paleocene-Eocene transition in inner neritic settings in Tunisia, similar to Gebel Duwi, Egypt. In addition, the

established foraminiferal isotopic record at Sidi Nasseur resembles the Tethyan values of the uppermost Paleocene at Gebel Duwi and Gebel Aweina. The latest Paleocene benthic $\delta^{13}C$ values of the NAS section are fairly stable and match well with contemporaneous deposits in Egypt. At the same time, $\delta^{18}O$ values suggest an upward increase in salinity.

Taking taphonomic alteration in consideration, our integrated study indicates that during the latest Paleocene,

the Sidi Nasseur section represented a shallow generally eutrophic inner neritic to coastal environment with open marine connections to the Tethys. Benthic assemblages are dominated by *Lenticulina* spp., *Anomalinoides midwayensis*, *Bulimina* spp. and non-calcareous agglutinated *Haplophragmoides* spp. Amongst the ostracodes trachyleberidid taxa dominate, in particular *Reymenticosta bensoni*. In general, the composition of the foraminiferal fauna points to stressed conditions at the seafloor, resulting from eutrophism and occasional low oxygen concentrations. During the latest Paleocene, the shallow water environment at Sidi Nasseur evolved to even shallower water depths with higher salinity and increasing dominance of *A. midwayensis*.

ACKNOWLEDGMENTS

We thank Mohadinne Ben Yahia for assistance in the field and Dr. Peter Schulte for logistic help with running stable isotopic analyses at Erlangen University. Simon D'Haenens and Kris Welkenhuysen (K.U.Leuven) are acknowledged for sample processing. Johan Yans (University of Namur) is thanked for his stimulating discussions. We thank Ellen Thomas (Yale University) and Michael Joachimski (University of Erlangen) for constructive comments on an earlier version of the manuscript. The K.U.Leuven Research Fund supported this research.

REFERENCES

- Aubert, J., Berggren, W.A., 1976. Paleocene benthic foraminiferal biostratigraphy and paleoecology of Tunisia. *Bulletin du Centre Recherches Pau-SNPA*, 10, 379-469.
- Aubry, M.-P., 1999. Late Paleocene-Early Eocene sedimentary history in western Cuba: Implications for the LPTM and for regional tectonic history. *Micropaleontology*, 45, Suppl. 2, 5-18.
- Bassiouni, M.A.A., Luger, P., 1990. Middle Eocene ostracoda from Northern Somalia. *Courier Forschungs Institut Senckenberg*, 129, 1-139.
- Bassiouni, M.A.A., Morsi, A. M., 2000. Paleocene-Lower Eocene ostracodes from El Quss Abu Said Plateau (Farafra Oasis), Western Desert, Egypt. *Palaeontographica A*, 257, 27-84.
- Bensalem, H., 2002. The Cretaceous-Paleogene transition in Tunisia: general overview. *Palaeogeography, Palaeoclimatology, Palaeoecology*, 178, 139-143.
- Berkeley, A., Perry, C.T., Smithers, S.G., Horton, B.P., Taylor, K.G., 2007. A review of the ecological and taphonomic controls on foraminiferal assemblage development in intertidal environments. *Earth-Science Reviews*, 83, 205-230.
- Berggren, W.A., 1974. Late Paleocene-Early Eocene benthonic foraminiferal biostratigraphy and paleoecology of Rockall Bank. *Micropaleontology*, 20, 426-448.
- Berggren, W.A., Kent, D.V., Swisher, C.C., Aubry, M.-P., 1995. A revised Cenozoic geochronology and chronostratigraphy. In: Berggren, W.A., Kent, D.V., Aubry, M.-P., Hardenbol, J. (eds.). *Geochronology, Time Scales and Global Stratigraphic Correlation*, 129-212.
- Berggren, W.A., Pearson, P.N., 2005. A revised tropical to subtropical Paleogene planktonic foraminiferal zonation. *Journal of Foraminiferal Research*, 35, 279-298.
- Bou Dagher, M., 1987. The Stainforthiidae (Foraminifera) in the late Palaeocene and early Eocene of Tunisia. *Bulletin des Centres de Recherches Exploration-Production Elf-Aquitaine*, 11, 133-152.
- Burollet, P.F., 1967. General Geology of Tunisia. Petroleum Exploration Society of Libya, 9th Annual Field Conference, Tripoli, 51-58.
- Charisi, S.D., Schmitz, B., 1998. Paleocene to early Eocene paleoceanography of the Middle East: The $\delta^{13}\text{C}$ and $\delta^{18}\text{O}$ isotopes from foraminiferal calcite. *Paleoceanography*, 13, 106-118.
- Dercourt, J., Gaetani, M., Vrielynck, B., Barrier, E., Biju-Duval, B., Brunet, M.F., Cadet, J.P., Crasquin, S., Sandulescu, M. (eds.), 2000. Atlas Peri-Tethys, Palaeogeographical Maps. Commission de la carte Géologique du Monde/Commission for the Geological maps of the World, Paris.
- Donze, P., Colin, J.-P., Damotte, R., Oertli, O., Peypouquet, J.-P., Said, R., 1982. Les ostracodes du Campanien terminal à l'Eocène inférieur de la coupe de Kef, Tunisie Nord-Occidentale. *Bulletin des Centres de Recherches Exploration-Production Elf-Aquitaine*, 6, 273-355.
- Dupuis, C., Steurbaut, E., Molina, E., Rauscher, R., Tribovillard, N., Arenillas, I., Arz, J.A., Robaszynski, F., Caron, M., Robin, E., Rocchia, R., Lefèvre, I., 2001. The Cretaceous-Palaeogene (K/P) boundary in the Ain Settara section (Kalaat Senan, Central Tunisia): lithological, micropalaeontological and geochemical evidence. *Bulletin Koninklijk Belgisch Instituut Natuurwetenschappen, Aardwetenschappen*, 71, 169-190.
- Dupuis, C., Aubry, M.-P., Steurbaut, E., Berggren, W.A., Ouda, K., Magioncalda, R., Cramer, B.S., Kent, D.V., Speijer, R.P., Heilmann-Clausen, C., 2003. The Dababiya Quarry section: lithostratigraphy, clay mineralogy, geochemistry and paleontology. In: Ouda, K., Aubry, M.-P. (eds.). *The Upper Paleocene-Lower Eocene of the Upper Nile Valley: Part 1, Stratigraphy*. *Micropaleontology*, 49, Suppl. 1, 41-59.
- Esker, G.C., 1968. Danian ostracodes from Tunisia. *Micropaleontology*, 14, 319-333.
- Ernst, S.R., Guasti, E., Dupuis, C., Speijer, R.P., 2006. Environmental perturbation in the southern Tethys across the Paleocene/Eocene boundary (Dababiya, Egypt): Foraminiferal and clay mineral records. *Marine Micropaleontology*, 60, 89-111.
- Guasti, E., Kouwenhoven, T.J., Brinkhuis, H., Speijer, R.P., 2005. Paleocene sea-level and productivity changes at the southern Tethyan margin (El Kef, Tunisia). *Marine Micropaleontology*, 55, 1-17.
- Guasti, E., Speijer, R.P., Brinkhuis, H., Smit, J., Steurbaut, E., 2006. Palaeoenvironmental change at the Danian-Selandi-

- an transition in Tunisia: Foraminifera, organic-walled dinoflagellate cyst and calcareous nannofossil records. *Marine Micropaleontology*, 56, 210-229.
- Kellough, 1965. Paleocology of the foraminiferida of the Wills Point Formation (Midway group) in northeast Texas. *Gulf Coast Association of Geological Societies*, 15, 73-153.
- Kouwenhoven, T.J., Speijer, R.P., van Oosterhout C.W.M., van der Zwaan, G.J., 1997. Benthic foraminiferal assemblages between two major extinction events: the Paleocene El Kef section, Tunisia. *Marine Micropaleontology*, 29, 105-127.
- Luger, P., 1985. Stratigraphie der marinen Oberkreide und des Alttertiärs im südwestlichen Oubnil-Becken (SW Ägypten) unter besonderer Berücksichtigung der Mikropaläontologie, Palökologie und Paläogeographie. *Berliner Geowissenschaftliche Abhandlungen. Reihe A. Geologie und Paläontologie* 63, 151 pp.
- Marshall, J.D., 1992. Climatic and oceanographic isotopic signals from the carbonate rock record and their preservation. *Geological Magazine*, 129, 143-160.
- Martini, E., 1971. Standard Tertiary and Quaternary calcareous nannoplankton zonation. *Proceeding of the II Planktonic Conference, Rome*, 739-785.
- Maslin, M.A., Swann, G.E.A., 2005. Isotopes in marine sediments. In: Leng, M.J. (Ed.), *Isotopes in Palaeoenvironmental Research*. Springer, 227-290.
- Morsi, A.M., 1999. Paleocene to Early Eocene ostracodes from the area of east-central Sinai, Egypt. *Revue de Paléobiologie*, 18, 31-55.
- Morsi, A.M., Speijer, R., 2003. High-resolution ostracode records of the Paleocene/Eocene transition in the South Eastern Desert of Egypt - Taxonomy, biostratigraphy, paleoecology and paleobiogeography. *Senckenbergiana Lethaea*, 83, 61-93.
- Murray, J.W., 1991. *Ecology and paleoecology of benthic foraminifera*. Harlow, Longman Scientific and Technical, 398 pp.
- Murray, J.W., Alve, E., 1999a. Natural dissolution of modern shallow water benthic foraminifera: taphonomic effects on the palaeoecological record. *Palaeogeography, Palaeoclimatology, Palaeoecology*, 146, 195-209.
- Murray, J.W., Alve, E., 1999b. Taphonomic experiments on marginal marine foraminiferal assemblages: how much ecological information is preserved? *Palaeogeography, Palaeoclimatology, Palaeoecology*, 149, 183-197.
- Nagy, J., Lødfaldi, M., Bäckström, S.A., 1988. Aspects of foraminiferal distribution and depositional conditions in middle Jurassic to early Cretaceous shales in Eastern Spitsbergen. In: Gradstein, F.M., Rögl, F. (eds.). *Second workshop on agglutinated foraminifera. Abhandlungen der Geologischen Bundesanstalt*, 41, 287-300.
- Pearson, P.N., Ditchfield, P.W., Singano, J., Harcourt-Brown, K.G., Nicholas, C.J., Olsson, R.K., Shackleton, N.J., Hall, M.A., 2001. Warm tropical sea surface temperatures in late Cretaceous and Eocene epochs. *Nature*, 413, 481-487.
- Peypouquet, J.-P., Grousset, F., Mourguiart, P., 1986. Paleooceanography of the Mesogean Sea based on ostracods of the northern Tunisian continental shelf between the Late Cretaceous and Early Paleogene. *Geologische Rundschau*, 75, 159-174.
- Pierre, C., Vergnaud-Grazzini, C., Thouron, D., Saliège, J.-F., 1986. Compositions isotopiques de l'oxygène et du carbone des masses d'eau en Méditerranée. *Mémoire de la Société géologique italienne*, 36, 165-174.
- Rohling, E.J., Bigg, G.R., 1998. Paleosalinity and $\delta^{18}\text{O}$: a critical assessment. *Journal of Geophysical Research*, 103, 1307-1318.
- Saint-Marc B., Berggren, W.A., 1988. A quantitative analysis of Paleocene benthic foraminiferal assemblages in Central Tunisia. *Journal of Foraminiferal Research*, 18, 97-113.
- Saint-Marc, P., 1992. Biogeographic and bathymetric distribution of benthic foraminifera in Paleocene El Haria Formation of Tunisia. *Journal of African Earth Sciences*, 15, 473-487.
- Schmitz, B., Speijer, R.P., Aubry, M.-P., 1996. Latest Paleocene benthic extinction event on the southern Tethyan shelf (Egypt): Foraminiferal stable isotopic ($\delta^{13}\text{C}$, $\delta^{18}\text{O}$) records. *Geology*, 24, 347-350.
- Schnack, K., 2000. *Biostratigraphie und fazielle Entwicklung in der Oberkreide und im Alttertiär im Bereich der Kharga Schwelle, Westliche Wüste, SW Ägypten*. *Berichte, Fachbereich Geowissenschaften, Universität Bremen*, 151.
- Shackleton, N.J., 1974. Attainment of isotopic equilibrium between ocean water and the benthic foraminifera Genus *Uvigerina*: isotope changes in the ocean during the last glacial. In: *Les méthodes quantitatives d'étude des variations due climat au cours du Pleistocene, Colloques Internationaux de Central National de la Recherche Scientifique (C.N.R.S.), Paris*, 219, 203-209.
- Speijer, R.P., 1994. Extinction and recovery patterns in benthic foraminiferal paleocommunities across the Cretaceous/Paleogene and Paleocene/Eocene boundaries. *Geologica Ultraiectina*, 124, 191 pp.
- Speijer, R.P., van der Zwaan, G.J., Schmitz, B., 1996. The impact of Paleocene/Eocene boundary events on middle neritic benthic foraminiferal assemblages from Egypt. *Marine Micropaleontology*, 28, 99-132.
- Speijer, R.P., Schmitz, B., 1998. A benthic foraminiferal record of Paleocene sea level and trophic/redox conditions at Gebel Aweina, Egypt. *Palaeogeography, Palaeoclimatology, Palaeoecology*, 137, 79-101.
- Speijer, R.P., Morsi, A.M., 2002. Ostracode turnover and sea-level changes associated with the Paleocene-Eocene thermal Maximum. *Geology*, 30, 23-26.
- Sturbaut, E., Dupuis, C., Arenillas, I., Molina, E., Matmati, M.F., 2000. The Kalaat Senan section in Central Tunisia: a potential reference section for the Danian/Selandian boundary. In: Schmitz, B., Sundquist, B., Andreasson, F.P. (eds.). *Early Paleogene Warm Climates and Biosphere Dynamics. GFF - The Geological Society of Sweden (Geologiska Föreningen)*, 122, 158-160.
- Thomas, E., 1998. Biogeography of the late Paleocene benthic foraminiferal extinction. In: Aubry, M.-P. et al. (eds.). *Late Paleocene-Eocene Climatic and Biotic Events in the Marine*

- and Terrestrial Records. New York, Columbia University Press, 214-243.
- Tjalsma, R.C., Lohmann, G.P., 1983. Paleocene-Eocene bathyal and abyssal benthic foraminifera from the Atlantic Ocean. *Micropaleontology*, Special publication, 4, 90 pp.
- Van der Zwaan, G.J., Jorissen, F.J., de Stigter, H.C., 1990. The depth dependency of planktonic/benthic foraminiferal ratios: Constraints and applications. *Marine Geology*, 95, 1-16.
- Van der Zwaan, G.J., Duijnste, I.A.P., den Dulk, M., Ernst, S.R., Jannink, N.T., Kouwenhoven T.J., 1999. Benthic foraminifera: proxies or problems? A review of paleoecological concepts. *Earth-Sciences Reviews*, 46, 213-236.
- Van Itterbeeck, J., Sprong, J., Dupuis, C., Speijer, R.P., Steurbaut, E., 2007. Danian/Selandian boundary stratigraphy and Ostracoda from Sidi Nasseur, Tunisia. *Marine Micropaleontology*, 62, 211-234.
- Youssef, M., 2003. Micropaleontological and stratigraphical analyses of the late Cretaceous/Early Tertiary succession of the Southern Nile Valley (Egypt). Doctoral thesis, University of Bochum, Germany, 197 pp.
- Zachos, J.C., Stott, L.D., Lohmann, K.C., 1994. Evolution of early Cenozoic marine temperatures. *Paleoceanography*, 9, 353-387.
- Zachos, J.C., Pagani, M., Sloan, L., Thomas, E., Billups, K., 2001. Trends, rhythms, and aberrations in global climate 65 Ma to present. *Science*, 292, 668-693.
- Zaïer, A., Beji-Sassi, A., Sassi, S., Moody, R.T.J., 1998. Basin evolution and deposition during the Early Paleogene in Tunisia. In: Macgregor, D.S., Moody, R.T.J., Clark Lowes (eds). *Petroleum Geology of North Africa*. The Geological Society of London, Special Publication, 132, 375-393.

**Manuscript received November 2007;
revision accepted May 2008;
published Online October 2008.**